Geosphere

Paleobathymetry and sequence stratigraphic interpretations from benthic foraminifera: Insights on New Jersey shelf architecture, IODP Expedition 313

Miriam E. Katz, James V. Browning, Kenneth G. Miller, Donald H. Monteverde, Gregory S. Mountain and Ross H. Williams

Geosphere published online 11 October 2013;
doi: 10.1130/GES00872.1

Notes

Paleobathymetry and sequence stratigraphic interpretations from benthic foraminifera: Insights on New Jersey shelf architecture, IODP Expedition 313

Miriam E. Katz[1], James V. Browning[2], Kenneth G. Miller[2], Donald H. Monteverde[2,3], Gregory S. Mountain[2], and Ross H. Williams[1,*]

[1]*Department of Earth and Environmental Sciences, Rensselaer Polytechnic Institute, 110 8th Street, Troy New York 12180, USA*
[2]*Department of Earth and Planetary Sciences, Rutgers University, Piscataway, New Jersey 08854, USA*
[3]*New Jersey Geological Survey, PO Box 427, Trenton New Jersey 07640, USA*

ABSTRACT

Integrated Ocean Drilling Program (IODP) Expedition 313 drilled three holes (Sites M27, M28, and M29; 34–36 m present water depth) across a series of prograding clinothems from the inner continental shelf of the New Jersey (USA) margin, a region that is sensitive to sea-level change. We examined 702 late Eocene to Miocene samples for benthic foraminiferal assemblages and planktonic foraminiferal abundances. We integrate our results with lithofacies to reconstruct paleobathymetry. Biofacies at all three sites indicate a long-term shallowing-upward trend as clinothems built seaward and sediment filled accommodation space. Patterns in biofacies and lithofacies indicate shallowing- and deepening-upward successions within individual sequences, providing the basis to recognize systems tracts, and therefore sequence stratigraphic relationships in early to early-middle Miocene sequences (ca. 23–13 Ma). The clinothem bottomsets and the lower portions of the foresets, which contain the thickest parts of clinothems, yield the deepest water biofacies. Shallower biofacies characterize the sequences in the upper portions of the clinothem foresets and on the topsets. Topsets are characterized by transgressive (TST) and highstand systems tracts (HST). Foresets contain lowstand systems tracts (LST), TSTs, and HSTs. Flooding surfaces mark parasequence boundaries within LSTs, TSTs, and HSTs. Superimposed on the long-term trends, short-term variations in paleowater depth are likely linked to global sea-level changes indicated by global oxygen isotopic variations.

INTRODUCTION

The New Jersey (USA) margin (Figs. 1 and 2) is an ideal setting for evaluating sequence stratigraphic principles and assumptions because it provides: (1) a thick accumulation of seismically imaged Oligocene to Holocene sediments (Poag, 1977; Schlee, 1981; Greenlee et al., 1988, 1992; Monteverde et al., 2008) that were deposited during a time of glacioeustatic oscillations (see Miller and Mountain, 1994; Austin et al., 1998); (2) a stable passive margin setting in a late stage of thermal cooling; (3) a mid-latitude location with excellent chronostratigraphic control; and (4) a substantial body of existing data ranging from seismic lines to wells to outcrops (see Mountain et al., 2010, for background on the transect). The New Jersey sea-level transect was designed to unravel the complex relationships between eustatic change and passive continental margin sedimentation. Studies from Ocean Drilling Program (ODP) Legs 150 (continental slope; Mountain et al., 1994) and 174A (outer continental shelf and slope; Austin et al., 1997) provided dates for the major sequence boundaries on the outermost shelf and upper slope. Onshore coastal plain studies from ODP Legs 150X and 174AX provided substantial detail of Late Cretaceous to Miocene sequences and facies (e.g., Miller et al., 2003). Integrated Ocean Drilling Program (IODP) Expedition 313 drilled a critical nearshore segment of the transect from the region that is most sensitive to sea-level change, the inner to middle continental shelf (Mountain et al., 2010). The goals of Expedition 313 focused on several aspects of sea-level change, including amplitude, sedimentary response, and related sequence stratigraphy.

Variations in global sea level (eustasy), tectonism, and sediment supply control the distribution of sediments, stratal geometries, and stacking patterns within depositional sequences on continental margins, especially on passive margins (Vail et al., 1977, 1991; Haq et al., 1987; Weimer and Posamentier, 1993; Christie-Blick and Driscoll, 1995). Mitchum et al. (1977, p. 53) defined a depositional sequence as a "stratigraphic unit composed of a relatively conformable succession of genetically related strata and bounded at its top and base by unconformities or their correlative conformities." The discipline of sequence stratigraphy was pioneered by Exxon Production Research Company (Exxon; Vail et al., 1977; Haq et al., 1987; Posamentier et al., 1988), which used it to extract eustatic records from passive margin sequences and to predict the facies distributions that control fluid resources. Exxon focused on eustasy as the primary genetic control, although this has been controversial (e.g., Christie-Blick et al., 1990; Miall, 1991) largely because distinguishing it from the many other processes that imprint continental margin records requires a wide range of data. Several studies have supported the chronology of the Exxon eustatic variations (e.g., Miller et al., 1996; Eberli et al., 1997), but the amplitude and shape of the Exxon curve have been shown to be incorrect (Christie-Blick et al., 1990; Miall, 1991; Miller et al., 1998, 2005). Despite this, Exxon documented that depositional sequences can be used objectively to partition the stratigraphic record. Exxon also provided several generations of depositional models for within-sequence facies variations, such as the systems tracts of Posamentier et al.

*Present address: Department of Earth, Atmospheric and Planetary Sciences, Massachusetts Institute of Technology, 77 Massachusetts Avenue, Cambridge, Massachusetts 02139-4307, USA.

Geosphere; December 2013; v. 9; no. 6; doi:10.1130/GES00872.1; 18 figures; 3 supplemental tables.
Received 11 October 2012 ♦ Revision received 20 July 2013 ♦ Accepted 4 September 2013 ♦ Published online 11 October 2013

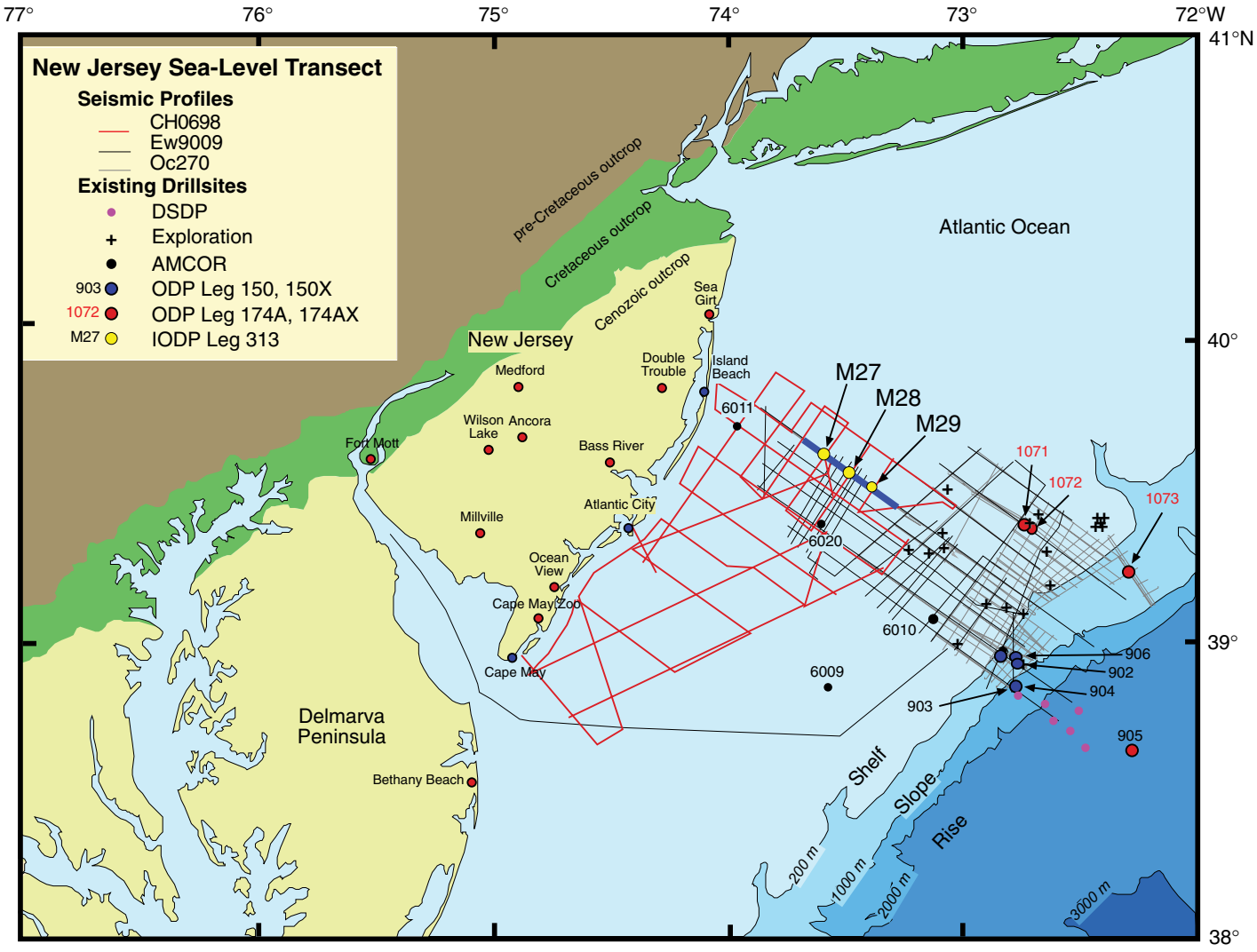

Figure 1. Generalized bathymetric location map of the New Jersey–Mid-Atlantic Margin sea-level transect showing three generations of multichannel seismic data (R/V *Ewing* cruise Ew9009, R/V *Oceanus* cruise Oc270, R/V *Cape Hatteras* cruise Ch0698), onshore coreholes, and offshore coreholes drilled by the Atlantic Margin Coring Program (AMCOR; Hathaway et al., 1979), Ocean Drilling Program (ODP), Integrated Ocean Drilling Program (IODP), and Deep Sea Drilling Project (DSDP). Modified after Mountain et al. (2010).

(1988). These depositional models have wide applicability (e.g., Winn et al., 1995; Abreu and Haddad, 1998; West et al., 1998), although many aspects of the models remain controversial or untested.

Many studies have applied the concept of systems tracts to sequence interpretations (e.g., Abbott and Carter, 1994; Kolla et al., 2000). However, few studies of offshore marine sections have continuously cored and logged sequences that display a classic clinothem geometry on a siliciclastic passive margin. Clinothems are packages of sediment generated by strata that prograde seaward into deeper water, and are bounded by surfaces (in this case sequence boundaries) with distinct sigmoidal (clinoform) shape. Clinothems have distinct topsets, foresets, and bottomsets (Fig. 2). Expedition 313 was designed to sample sequences in all three settings.

Paleobathymetric trends of shallowing and deepening can be used to identify systems tracts (Fig. 2, inset). Identifying the vertical succession of benthic foraminiferal biofacies and interpreting those changes with regard to paleobathymetric changes (e.g., Natland, 1933; Bandy, 1960) is a critical component of recognizing systems tracts. Planktonic foraminiferal abundance changes provide an additional proxy for water depth variations (e.g., Grimsdale and van Morkhoven, 1955); higher abundances typically indicate deeper waters, although this index can be influenced by other effects (e.g., productivity and dissolution).

Lithofacies variations can also provide a basis for interpreting paleoenvironmental changes; for example, clays and silts tend to dominate low-energy environments, whereas sands tend to characterize higher energy environments. However, lithofacies are rarely environmentally unique, and thus paleoenvironmental interpretations based on lithofacies alone can be incorrect. Nonetheless, Expedition 313 used an effective wave-dominated shoreline model for depths <30 m that recognized upper shoreface (0–5 m), lower shoreface (5–10 m), shoreface-offshore transition (10 to 20–30 m), and offshore (>20–30 m) environments, with excellent paleodepth resolution (±5 m) (summarized in Mountain et al., 2010). Lithofacies are usually insufficient for estimating paleodepths deeper than

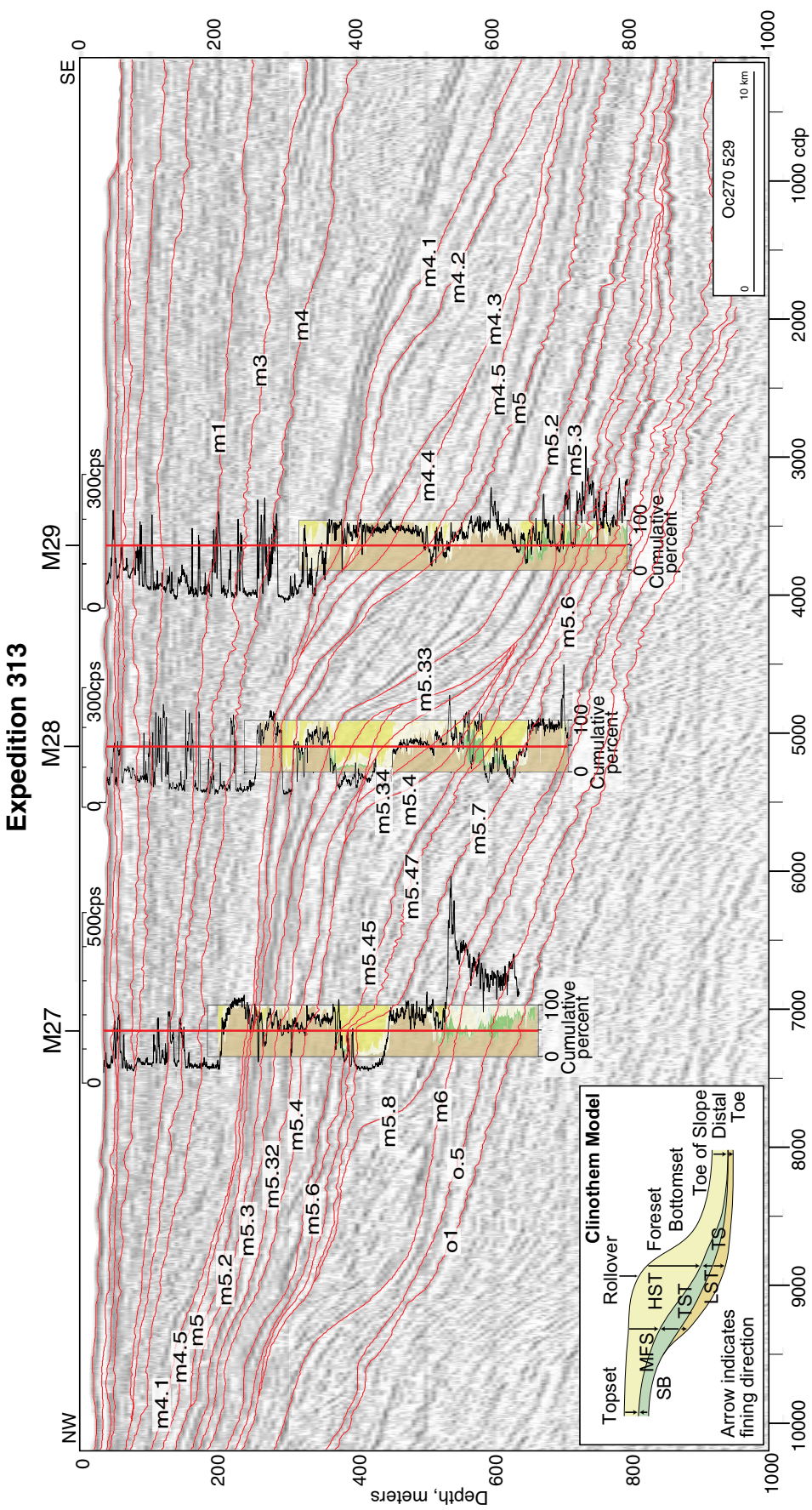

Figure 2. Multichannel seismic line Oc270 529 (R/V *Oceanus* cruise Oc270) in the region of Integrated Ocean Drilling Program Expedition 313 collected along dip profile from northwest to southeast. Sites M27–M29 are located on this line (modified after Mountain et al., 2010). Axes are depth in meters obtained using the revised velocity-depth function (Mountain and Monteverde, 2012) and common depth points (cdp); approximate scale (in km) is given on lower right. Major seismic sequence boundaries and select intrasequence reflectors (o1, o.5, m5.34-m5.32) are shown; all others are seismic sequence boundaries (m4.1 is a merged TS and sequence boundary in this area). The lithologic cumulative percentage plots (Miller et al., 2013a) and downhole gamma logs (in counts per second, cps) (Mountain et al., 2010) are superimposed on the profile. Inset is a generalized clinothem model. TS—transgressive surface; TST—transgressive systems tract; LST—lowstand systems tract; HST—highstand systems tract; MFS—maximum flooding surface; SB—sequence boundary.

shoreface-offshore transition facies (>30 m). The reliability of paleoenvironmental interpretations can be greatly improved by integrating biofacies and lithofacies analyses (Fig. 3), viewed within the seismic stratigraphic framework.

In this paper, we use IODP Expedition 313 drilling results (Mountain et al., 2010) from late Eocene to Miocene sequences to link microfaunal and sedimentologic data with prograding clinoform geometries on the inner continental shelf of the New Jersey passive margin. Specifically, we document the benthic foraminiferal assemblages and planktonic foraminiferal abundances at Sites M27, M28, and M29 (Figs. 1 and 2). We integrate the foraminiferal data with chronostratigraphy (Browning et al., 2013), lithofacies, seismic stratigraphy, and downhole logs (Miller et al., 2013a; Inwood et al., 2013) to produce paleobathymetric reconstructions within a seismic stratigraphic framework. We integrate these studies to interpret systems tracts and sequence stratigraphy.

METHODS

Biofacies

Samples were soaked overnight in a sodium metaphosphate solution made with deionized water (5.5 g/L) and then washed with tap water through a 63 µm sieve and oven-dried at ~50 °C overnight. We analyzed a total of 702 samples from the 3 Expedition 313 sites; 271 samples yielded benthic foraminifera, 427 samples were barren, and 4 samples contained planktonic (but no benthic) foraminifera. Sample resolution is typically 1–3 m (1–3 samples/3 m core). Higher resolution samples (~4–10 cm intervals) were analyzed around some sequence boundaries and lithology changes.

Foraminifera were picked from the >150 µm fraction because previous studies used for comparisons (e.g., Olsson et al., 1987; Miller et al., 1997) were based on data sets that used the >150 µm fraction. The 63–150 µm fraction was not quantitatively picked for this study, although it was observed that foraminifera typically were rare or absent in the 63–150 µm fraction, which may indicate dissolution or winnowing. Using a sample splitter, samples were split to a size that targeted ~100 specimens per aliquot. Samples with as few as 20 specimens were included in the multivariate analyses (see following). Some very large samples (>20 g) yielded sparse benthic foraminifera (i.e., with too few specimens to be included in multivariate analyses) and very low diversity (or even monospecific) assemblages lacking depth-diagnostic taxa (e.g., dominated by large *Lenticulina* spp.). In these cases, a split was picked, and then the rest of the sample was scanned to confirm the low diversity or monospecific nature of the sample, because picking that entire sample would not meaningfully alter the result, but was time consuming.

We performed Q-mode varimax factor analyses on the relative abundance (percentage) data using Systat Software (www.systat.com) SYSTAT version 5.2.1. The Q-mode varimax factor program utilizes a cosine-theta matrix, standardizing each sample to unit length. Samples load onto a sample-defined vector in these Q-mode analyses. We chose this method over other methods because it yielded useful results in studies that we use for comparison (e.g., Miller et al., 1997; Pekar et al., 1997), and our results are consistent with these studies. Each of the 3 sites was analyzed separately, and all samples with at least 20 specimens were included in the factor analysis, which is lower than the 50 specimen cutoff used in Miller et al. (1997). The 20 specimens per sample cutoff is extremely low, even for high-dominance low-diversity assemblages typical of shelf assemblages (e.g., Murray, 1991; Miller et al., 1997). We note that only 21 samples have 20–49 specimens (8 at Site M27, 4 at Site M28, and 9 at Site M29). Of these 21 samples, only 2 yield factor analysis and abundance results that are inconsistent with surrounding samples. One of these samples contains 100% *Lenticulina* spp. and is not used in the paleobathymetric interpretation. The other sample indicates a paleodepth change at Site M27 that is consistent with a well-constrained paleobathymetric change at Site M29 in the same sequence (see Discussion), and therefore is used in the paleobathymetric reconstruction.

Taxonomic concepts were drawn from multiple references (Cushman and Cahill, 1933; Gibson, 1983; Schnitker, 1970; Boersma, 1984; Snyder et al., 1988; Parker, 1948; Poag, 1988; van Morkhoven et al., 1986; see these for taxonomic details and illustrations of species identified in this study). In addition, Expedition 313 specimens were compared with samples from our previous studies (Miller et al., 1997; Katz et al., 2003a) and with type specimens archived at the National Museum of Natural History (Smithsonian Institution, Washington, D.C.). To supplement the detailed information provided in the preceding citations, we offer notes for identifying certain species.

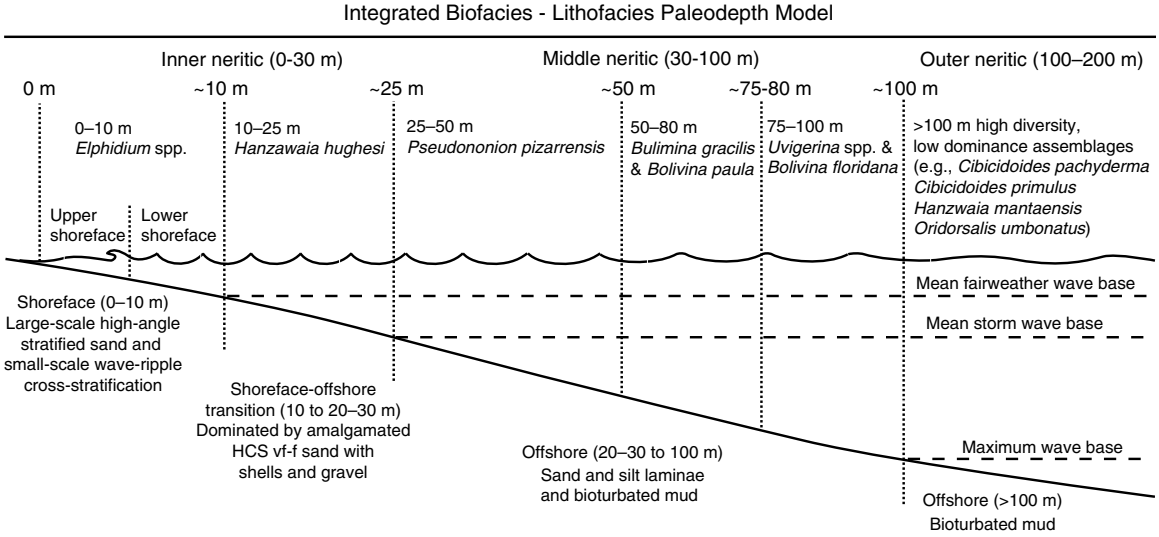

Figure 3. Integrated biofacies and lithofacies paleodepth model. Major benthic foraminiferal species from this study are added to the biofacies model of Miller et al. (1997) and lithofacies model of Mountain et al. (2010). HCS—hummocky cross-stratification; vf—very fine; f—fine.

The holotype of *Bulimina gracilis* is elongated with an overall twist in the test. *B. elongata* is essentially the same as *B. gracilis* but without the twist, and with a small curvature. Paratypes of *B. gracilis* vary in the degree of elongation and of twist; in fact, some completely lack a twist. The holotype of *B. elongata* is missing, so a direct comparison to *B. gracilis* could not be made. Some specimens from Expedition 313 samples display the two end-member morphologies of *B. gracilis* and *B. elongata*, but most range from elongated to short, and vary in degree of twist and curvature, with no clear dividing line between the two species morphologies. They tend to co-occur, and do not appear to indicate different environments; therefore, we combine them under the name *B. gracilis*.

Buliminella curta is distinct from *B. gracilis*. The chamber length to width ratio is consistently higher in *B. curta*, resulting in vertically elongated chambers compared to the chambers of *B. gracilis*; this distinction places the two species in different genera. The sutures between chambers are slightly more depressed in *B. gracilis*, giving the chambers a somewhat puffier look than in *B. curta*. *B. curta* tests are distinctively twisted, without the variability seen in *Bulimina gracilis/elongata*. The combination of the test twist, longer chambers, and the smoother, flatter transition between chambers gives *B. curta* a morphology that is distinct from *Bulimina gracilis/elongata*.

Several species of *Uvigerina* are abundant in many of the Expedition 313 samples. Holotypes and paratypes of species named in studies of the eastern U.S. continental margin were examined at the Smithsonian, including *U. subperegrina*, *U. calvertensis*, *U. juncea*, and *U. modeloensis*. *U. subperegrina* is entirely costate, with relatively large costae. Compared to *U. subperegrina*, *U. calvertensis* and *U. juncea* have finer costae, more elongate tests, and final chambers that are sometimes finely hispid with or without fine costae, or even nearly smooth. *U. modeloensis* is nearly entirely smooth, with very faint striae sometimes visible. Some specimens display the end-member morphologies of the various *Uvigerina* species in Expedition 313 samples, but many show intermediate morphologies that are not readily distinguishable, with no clear dividing line among the different species. Therefore, we combined them for the factor analyses and abundance plots.

Paleobathymetry

Benthic foraminifera are the only seafloor-dwelling microfossils that occur consistently in Expedition 313 marine facies, providing the best means to reconstruct paleobathymetry. Different benthic foraminiferal species typically colonize certain water depth ranges, with key depth-indicator species providing an invaluable tool for reconstructing paleobathymetry (e.g., Olsson et al., 1987; Browning et al., 1997; Miller et al., 1997; Pekar et al., 1997; Katz et al. 2003a). Therefore, the paleodepth history of a site can be determined by documenting benthic foraminiferal changes through time. In addition, higher planktonic foraminiferal abundances typically indicate deeper waters (Grimsdale and van Morkhoven, 1955). Patterns in foraminiferal data indicate shallowing- and deepening-upward successions within a sequence. In addition, lithologic trends are important in reconstructing paleodepth history. The Expedition 313 sedimentologists produced visual core descriptions and differentiated clay, silt, and various sand fractions visually and using smear slides (Mountain et al., 2010). In Miller et al. (2013a), quantitative and qualitative lithology data were added; weight percent mud (<63 μm), fine to very fine sand (63–250 μm), and medium sand and coarser sediment (>250 μm) were measured, and semiquantitative estimates made of the abundances of glauconite, shells, and mica in the sand fraction. Water depth trends determined from foraminifera (e.g., deepening-upward transgressive and shallowing-upward regressive successions) combined with water depth trends inferred from sedimentology (grain-size changes and facies analysis) can be used to infer systems tracts and hence sequence stratigraphic relationships (see inset, Fig. 2).

At the Expedition 313 sites, paleobathymetric ranges were based primarily on benthic foraminiferal biofacies determined from factor analysis, with the highest loading factor taking precedence; a broader depth range was assigned when the two highest factors yielded approximately the same loadings. Within this framework, paleodepths were fine-tuned using abundances of key depth-indicator taxa, supplemented by planktonic foraminiferal relative abundances. We note that species abundances in samples with few specimens were not used to fine-tune factor analysis results. In general, the low-diversity and high-dominance benthic foraminiferal assemblages in the Expedition 313 boreholes are marked by biofacies that are dominated by 1–3 species or genera; this is typical of shallow-water shelf environments (e.g., Murray, 1991; Miller et al., 1997).

A paleobathymetric calibration for benthic foraminiferal biofacies was established in Miller et al. (1997), using the paleoslope model of Olsson et al. (1987) for Miocene sequences drilled on the New Jersey coastal plain. The paleoslope model method has been used successfully for New Jersey coastal plain sequences of different ages (e.g., Browning et al., 1997; Pekar et al., 1997), and is based on Walther's Law (lateral biofacies variations are also expressed as vertical variations). This method uses a paleoslope of 1:1000, calculated using two-dimensional (2-D) backstripping (Steckler et al., 1999), and equivalent to the modern slope in New Jersey. Boreholes are projected along strike to place them on a common dip line, vertical offsets among the boreholes are determined, and biofacies differences are documented for the same age samples at the different boreholes. This allows coeval biofacies to be linked within sequences. Lithofacies models place additional constraints on shallower biofacies. For example, inner neritic (<30 m) environments recognized using biofacies can be further subdivided into foreshore (<5 m), upper shoreface (~5–10 m), and lower shoreface to shoreface–offshore transition (10 to 20–30 m) environments (Mountain et al., 2010). We compare our results to distance from shoreline estimates that are based on the abundances of marine versus terrestrial palynomorphs (McCarthy et al., 2013). In addition to variations in sea surface productivity, terrestrial and marine palynomorph abundances are related mechanisms that transport pollen and embryophyte spores offshore, including wind, rivers, ocean currents, and downslope transport, most of which are related to distance from shoreline.

Bathymetric zones are defined as inner neritic (0–30 m), middle neritic (30–100 m), and outer neritic (100–200 m) (van Morkhoven et al., 1986). In Miller et al. (1997), these zones were subdivided on the New Jersey margin when they interpreted *Elphidium*-dominated biofacies as upper inner neritic (<10 m), *Hanzawaia hughesi*–dominated biofacies as mid-inner neritic (10–25 m), *Pseudononion pizarrensis*–dominated biofacies as lower inner neritic to upper middle neritic (25–50 m), *B. gracilis*–dominated biofacies as middle middle neritic (50–80 m), and *Uvigerina*-dominated biofacies as outer middle neritic (>75 m). The absence of *Elphidium* in our samples may indicate a different paleoenvironmental setting than in the Miller et al. (1997) study, or dissolution in the shallowest water environments (<10 m) at the Expedition 313 sites. Alternatively, *Elphidium* may be present in interbeds of mud in shoreface sediments that were not sampled.

We build on the paleobathymetric calibrations for benthic foraminiferal biofacies established using the paleoslope method for New Jersey coastal plain Miocene sequences (Miller et al., 1997) as follows (Fig. 3). *Lenticulina* spp. (and/or the related *Astacolus dubius*) is common

in many samples and was delineated by factor analysis at all three Expedition 313 sites. *Lenticulina* spp. is found from the inner shelf to the deep sea through the Cenozoic (e.g., Culver and Buzas, 1980; Katz et al., 2003b; Miller and Katz, 1987; Speijer et al., 1996; Tjalsma and Lohmann, 1983), and therefore is not a useful depth indicator. Four isolated samples yielding several planktonic foraminifera, but no benthic foraminifera, must have been deposited in a marine setting, and were assigned a paleodepth of at least 0–10 m, but were not used in the paleobathymetric interpretation (1 sample at Site M27, 1 sample at Site M28, and 2 samples at Site M29) (Supplemental Table 1[1]).

Based on factor analyses, we identify several additional depth-diagnostic species that can be used in paleobathymetric reconstructions. *Bolivina paula* is associated with *B. gracilis*, indicating 50–80 m paleodepths in this region (see following discussion of Site M29). Similarly, *B. floridana* is associated with *Uvigerina* spp., and therefore is also is indicative of 75–100 m paleodepths in this region (see following discussion of Site M28).

For deeper biofacies not recovered by Miller et al. (1997), we use key taxa (e.g., *Cibicidoides pachyderma*, *Cibicidoides primulus*, *H. mantaensis*, *Oridorsalis umbonatus*) often found in high-diversity, low-dominance assemblages that indicate outer neritic paleodepths (100–200 m; e.g., Katz et al., 2003a; Parker, 1948; Poag, 1981; van Morkhoven et al., 1986). Because changes from the *Uvigerina* spp. biofacies to the deeper biofacies occur gradually within sequences, we infer that the maximum water depths are in the shallower part of the outer neritic zone (~120 m).

Paleobathymetric reconstructions in paleoshelf settings (such as drilled by Expedition 313) can be hampered by samples dominated by coarse sediment that are devoid of foraminifera. These barren sediments may be in situ mid-shelf sands, in situ extremely shallow-water deposits, or transported shallow-water and/or terrigenous sediments. Alternatively, all foraminifera may have been dissolved out of the barren intervals, typically in prodelta shoreface, river-influenced offshore, and bottom-of-slope coarse-grained sediments (see following). Because we cannot distinguish among these possibilities, barren intervals of ~10 m or greater are left blank in the paleobathymetric reconstruction figures, and no paleodepth estimate is made for isolated barren samples or thin barren intervals. The sample coverage in these barren intervals is indicated in the figures and in Supplemental Table 1 (see footnote 1), Supplemental Table 2[2], and Supplemental Table 3[3].

Age Control and Sequence Boundaries

Ages, sequence boundaries, and intrasequence surfaces used in this paper build on the work in Mountain et al. (2010). All ages provided in this study are from the chronostratigraphy in Browning et al. (2013), wherein latest Eocene to middle Miocene sequences at Sites M27, M28, and M29 were dated using integrated biostratigraphy (primarily calcareous nannoplankton, diatoms, and dinocysts) and strontium isotopic stratigraphy. In general, the age resolution is ±0.5 m.y., and is as good as ±0.25 m.y. in many sequences.

All identifications of sequence boundaries and intrasequence surfaces are from Miller et al. (2013a), based on an integrated study of core surfaces, lithostratigraphy and process sedimentology (grain size, mineralogy, facies, and paleoenvironments), facies successions, stacking patterns, benthic foraminiferal water depths, downhole logs, core gamma logs, and chronostratigraphic ages. The sequence boundaries and surfaces are identified based on integration of seismic profiles, core surfaces, lithostratigraphy (grain size, mineralogy, facies, and paleoenvironments), facies and biofacies successions, downhole and core gamma logs, and chronostratigraphic ages.

Paleobathymetric Reconstructions and Sequence Stratigraphy

We use benthic and planktonic foraminiferal evidence, integrated with lithologic and seismic evidence, to delineate shallowing- and deepening-upward successions as our primary means of recognizing systems tracts. Each systems tract is marked at its base and its top by a key surface that is defined by its stratal (seismic, log, and core) character. By placing these surfaces with a seismic resolution of 5 m, we can then interpret facies changes within sequences and more accurately locate these important stratal boundaries. Sequences are separated by sequence boundaries. Sequence boundaries are recognized on seismic lines by classic criteria of onlap, toplap, downlap, and erosional truncation (Mitchum et al., 1977). Sequence boundaries are recognized in cores by the criteria outlined in Miller et al. (2013a). The transgressive systems tract (TST) is recognized by a deepening-upward facies succession that is bounded by a transgressive surface (TS) below and a maximum flooding surface (MFS) above (Posamentier et al., 1988). MFSs are often identified as downlap surfaces on seismic profiles and omission surfaces in cores; however, the placement of a MFS is often ambiguous, using seismic or lithofacies criteria. Benthic foraminifera and abundances of planktonic foraminifera often provide the strongest evidence for the greatest water depths associated with MFSs landward of the rollover, although often these are zones rather than distinct surfaces (Loutit et al., 1988). Changes from deepening-upward (retrogradational) to shallowing-upward (progradational) successions are used to identify MFSs (Fig. 2, inset; Posamentier and Vail, 1988; Neal and Abreu, 2011; Miller et al., 2013b). MFSs normally mark the deepest water depths in a sequence and are associated with peaks in percent planktonic foraminifera, heavy bioturbation, and, in some cases, authigenic deposits (in situ glauconite and phosphorites; Loutit et al., 1988). Seaward of this, deep-water benthic foraminifera occur on the bottomsets, but often display no clear trends and identification of the MFS is not possible.

The highstand systems tract (HST) overlies the MFS and shallows upward to the overlying sequence boundary (Posamentier et al., 1988). In our interpretations, for example, an intrasequence succession of shallowing-upward foraminifera overlain by deepening-upward foraminifera indicates lowstand systems tract (LST) deposits transitioning to, or overlain by, TST deposits. Sedimentological criteria typically support water depth inferences derived from foraminifera; for example, LSTs tend to coarsen upsection, TSTs tend to fine upsection, and HSTs tend to coarsen upsection (Fig. 2, inset). This integrated approach has been used in previous studies of the New Jersey margin transect from the coastal plain to the continental slope (e.g., Olsson et al., 1987; Miller et al., 1997; Pekar et al., 1997; Browning et al., 1997; Katz et al., 2003a). An important additional step is to integrate stratal architecture with the biofacies and lithofacies of the Expedition 313 sections, a task attempted for sequences m5.8, m5.4, and m5.2 in Miller et al. (2013b); sequences m5.8 and m5.2 appear to be single million-year-scale sequences, whereas sequence m5.4 is a composite of three higher frequency sequences.

[1]Supplemental Table 1. Site M27 foraminiferal data. If you are viewing the PDF of this paper or reading it offline, please visit http://dx.doi.org/10.1130/GES00872.S1 or the full-text article on www.gsapubs.org to view Supplemental Table 1.

[2]Supplemental Table 2. Site M28 foraminiferal data. If you are viewing the PDF of this paper or reading it offline, please visit http://dx.doi.org/10.1130/GES00872.S2 or the full-text article on www.gsapubs.org to view Supplemental Table 2.

[3]Supplemental Table 3. Site M29 foraminiferal data. If you are viewing the PDF of this paper or reading it offline, please visit http://dx.doi.org/10.1130/GES00872.S3 or the full-text article on www.gsapubs.org to view Supplemental Table 3.

The LST can be recognized as a regressive deposit between a sequence boundary and an overlying TS (Posamentier et al., 1988) typically preserved on a foreset (Fig. 2, inset; Miller et al., 2013b), but LSTs are more difficult to recognize in shelf boreholes using paleontological criteria alone (Katz et al., 2003a). LST sediments often consist of reworked coarse sediments containing transported shallow-water foraminifera. It can be difficult to differentiate shallow-water in situ foraminifera from shallow-water transported foraminifera. Although usually deposited in deeper water, LST deposits can resemble shoreface sands. We rely on the presence of deeper water indicators or abundant reworked (damaged) specimens to differentiate shallow- from deep-water sands. In general, LSTs should shallow upward due to progradation or show relatively constant water depths during aggradation (Posamentier et al., 1988).

We use integrated benthic and planktonic foraminiferal biofacies, lithofacies, and seismic evidence as the primary basis for reconstructing paleobathymetry and recognizing systems tracts, providing constraints on the prograding clinothems sampled at each site. This is done to the fullest extent that we are able to do without conducting: (1) 1-D backstripping, a technique used to account for compaction, loading, and thermal subsidence (Kominz et al., 2008); and (2) 2-D backstripping, a technique that also accounts for flexural rigidity between locations and provides an estimate of paleotopography (Steckler et al., 1999).

RESULTS

Site by Site Biofacies

Site M27

We examined 206 samples from Site M27 (Figs. 4–6; Supplemental Table 1 [see footnote 1]). Q-mode analysis was based on 75 taxa and 72 samples, with 83.34% of the variance explained by 5 factors (Fig. 4). Factor 1 accounts for 18.28% of the total variance and is characterized by *B. gracilis*, indicating paleodepths of ~50–80 m. Factor 2 (19.26% of the total variance) is characterized by *Lenticulina* spp. Factor 3 (20.52% of the total variance) is characterized by *P. pizarrensis* (25–50 m), *Hanzawaia* sp. 1, and *H. hughesi* (10–25 m). Factor 4 (10.43% of the total variance) is characterized by *C. primulus* and *Gyroidinoides* spp. (>100 m). Factor 5 accounts for 14.85% of the total variance, and is characterized by *Uvigerina* spp. (*U. calvertensis*, *U. juncea*, *U. modeloensis*, and *U. subperegrina*) and *Gyroidinoides* spp. (75–100 m).

Factor analysis indicates that there is an overall paleobathymetric shallowing upsection (Fig. 6), from 100 to 120 m (~630–620 m composite depth, mcd), to 75–100 m (~600–500 mcd), to 50–80 m (~470–420 mcd), to 25–50 m with sporadic deeper facies (~335–200 mcd). Within this long-term trend, there are depth variations within the sequences that are discussed in the following sections.

Site M28

We examined 224 samples from Site M28 (Figs. 7–9; Supplemental Table 2 [see footnote 2]). Many samples below ~400 mcd were

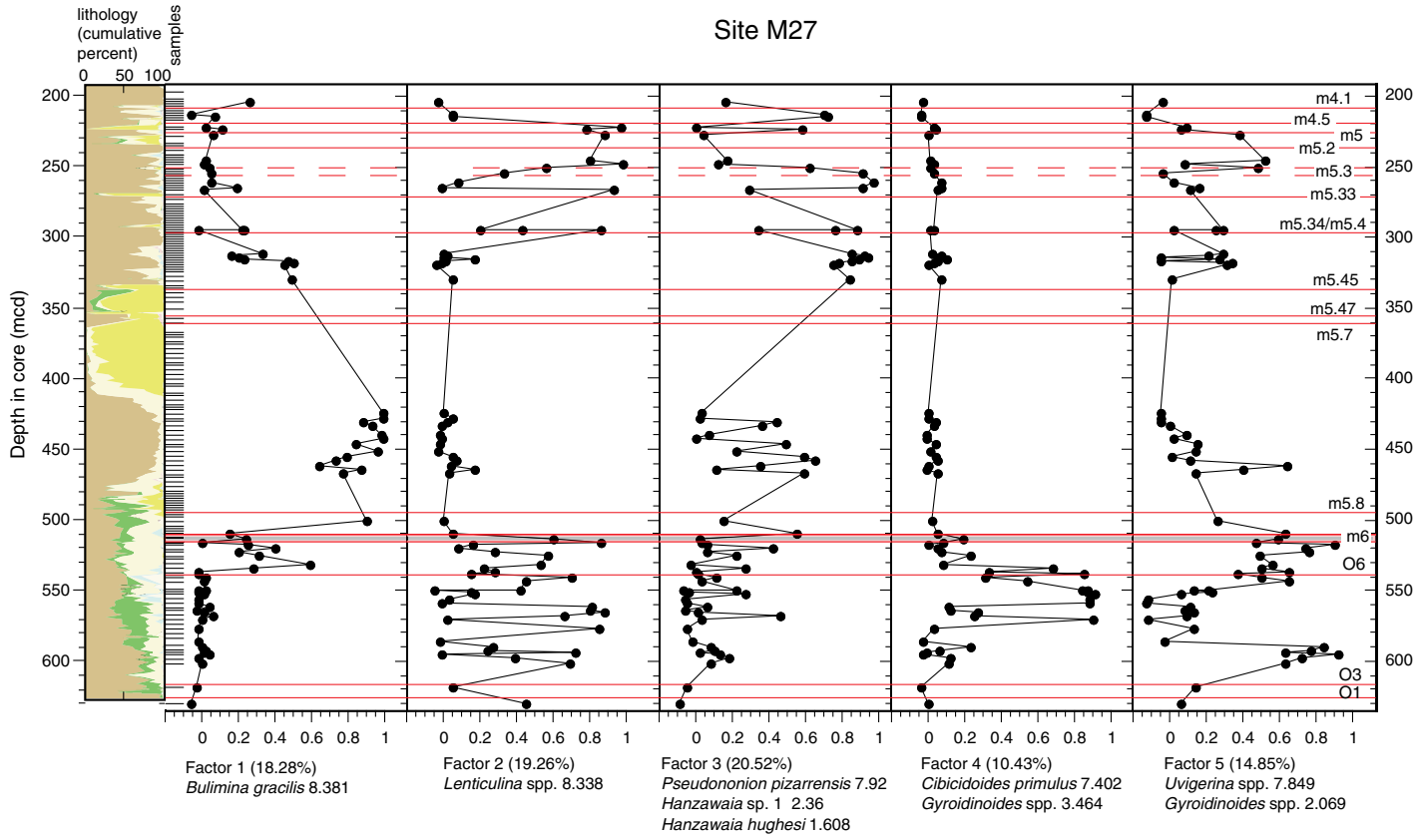

Figure 4. Integrated Ocean Drilling Program Expedition 313 Site M27 factors within the sequence stratigraphic framework (mcd—meters composite depth). Samples examined for benthic foraminifera are indicated in the samples column. Species that characterize each factor are shown with the factor scores, along with the variance explained by each factor. The cumulative percentage plot shows lithology (Miller et al., 2013a). Brown—mud; light yellow—fine quartz sand; dark yellow—medium-coarse quartz sand; green—glauconite sand; blue—carbonate (shells and foraminifera).

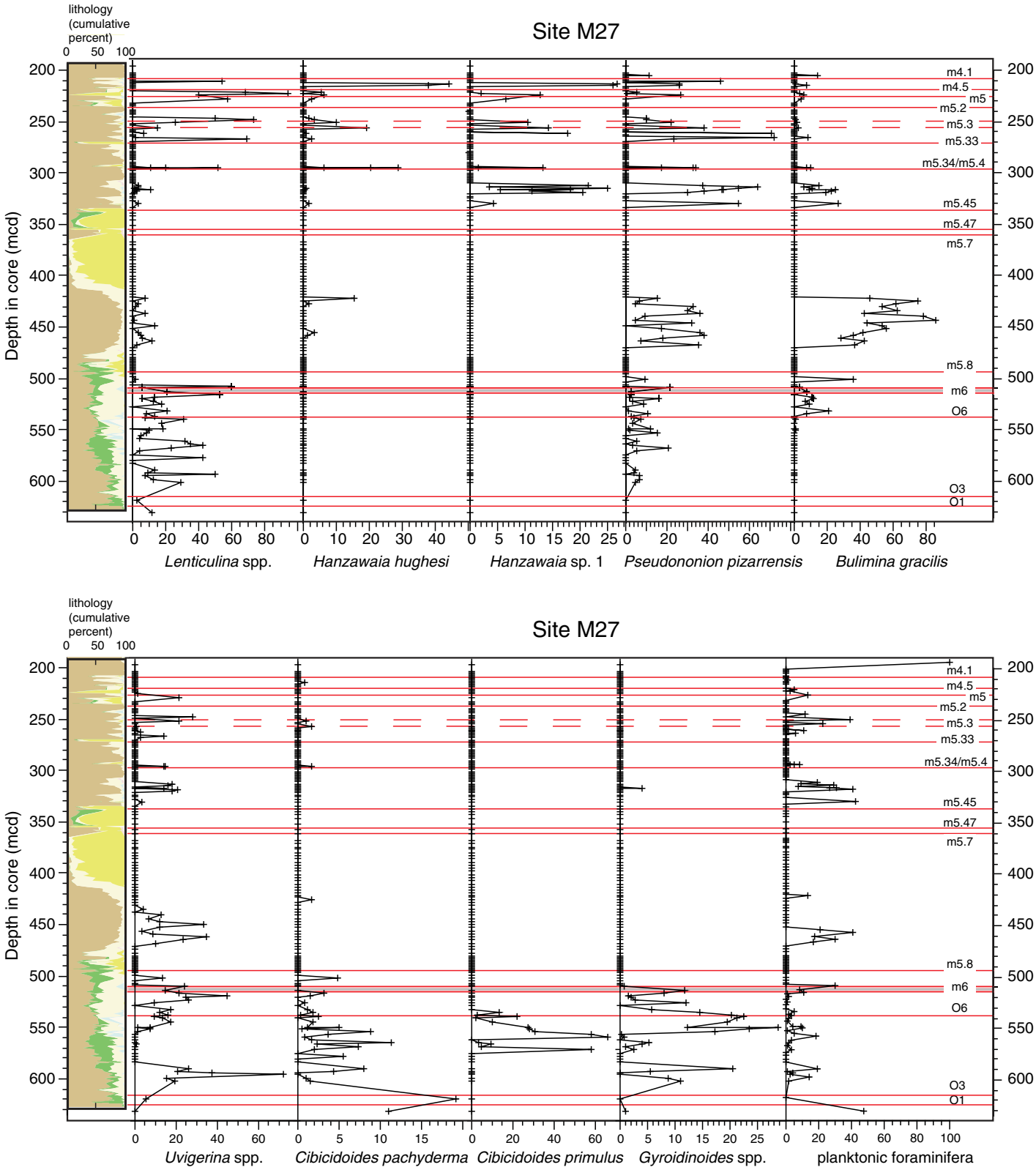

Figure 5. Integrated Ocean Drilling Program Expedition 313 Site M27 relative abundances (percentages) of dominant species delineated by factor analysis, along with percentage of planktonic foraminifera, shown within the sequence stratigraphic framework (mcd—meters composite depth). Samples examined for benthic foraminifera are indicated in the samples column. The cumulative percentage plot shows lithology (Miller et al., 2013a). Brown—mud; light yellow—fine quartz sand; dark yellow—medium-coarse quartz sand; green—glauconite sand; blue—carbonate (shells and foraminifera).

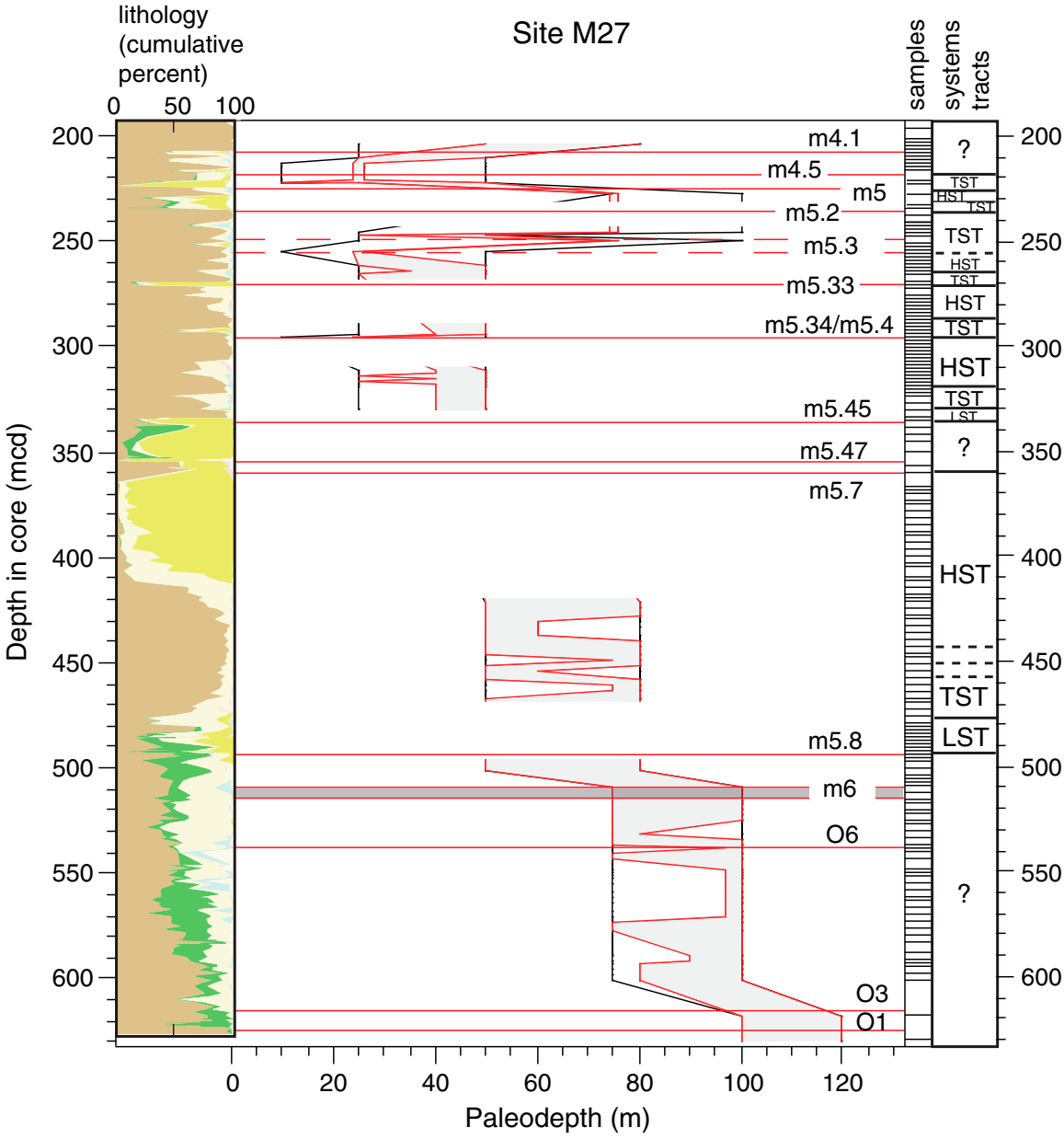

Figure 6. Integrated Ocean Drilling Program Expedition 313 Site M27 paleodepths are estimated from benthic foraminifera and shown within the sequence stratigraphic framework (mcd—meters composite depth). Shaded swath is best estimate; black envelope indicates possible paleodepth range. Systems tracts interpretations are shown. TST—transgressive systems tract; LST—lowstand systems tract; HST—highstand systems tract. The cumulative percentage plot shows lithology (Miller et al., 2013a). Brown—mud; light yellow—fine quartz sand; dark yellow—medium-coarse quartz sand; green—glauconite sand; blue—carbonate (shells and foraminifera).

barren; below ~500 mcd, nearly all samples were barren. Q-mode analysis was based on 45 taxa and 34 samples, with 96.53% of the variance explained by 5 factors (Fig. 7–9). Factor 1 accounts for 35.51% of the total variance, and is characterized by *H. hughesi* (10–25 m). Factor 2 (30.60% of the total variance) is characterized by *Lenticulina* spp. Factor 3 (10.18% of the total variance) is characterized by *Uvigerina* spp. (*U. calvertensis*, *U. juncea*, *U. modeloensis*, and *U. subperegrina*) and *B. floridana* (75–100 m). Factor 4 accounts for 12.50% of the total variance, and is characterized by *A. dubius* and *Lenticulina* spp. Factor 5 accounts for 7.58% of the total variance, and is characterized by *P. pizarrensis* (25–50 m) and *B. gracilis* (50–80 m).

Factor analysis indicates that there is an overall paleobathymetric shallowing upsection (Fig. 9), from 75 to 100 m (~500–475 mcd), to 50–60 m (~430 mcd), to 0–25 m (~390–270 mcd).

Site M29

We examined 272 samples from Site M29 (Figs. 10–12; Supplemental Table 3 [see footnote 3]). Q-mode analysis was based on 60 taxa and 121 samples, with 89.91% of the

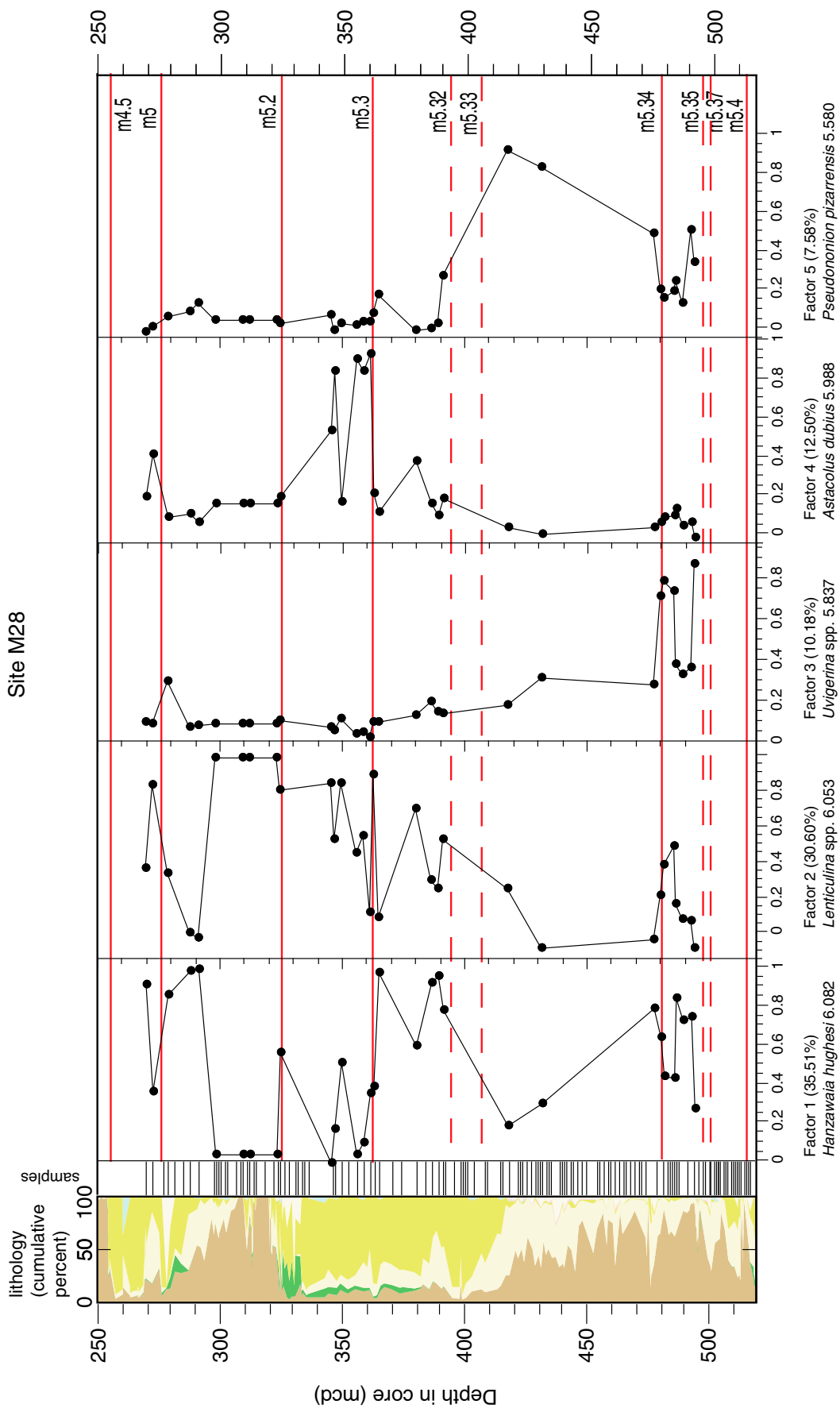

Figure 7. Integrated Ocean Drilling Program Expedition 313 Site M28 factors within the sequence stratigraphic framework (mcd—meters composite depth). Samples examined for benthic foraminifera are indicated in the samples column. Species that characterize each factor are shown with the factor scores, along with the variance explained by each factor. The cumulative percentage plot shows lithology (Miller et al., 2013a). Brown—mud; light yellow—fine quartz sand; dark yellow—medium-coarse quartz sand; green—glauconite sand; blue—carbonate (shells and foraminifera).

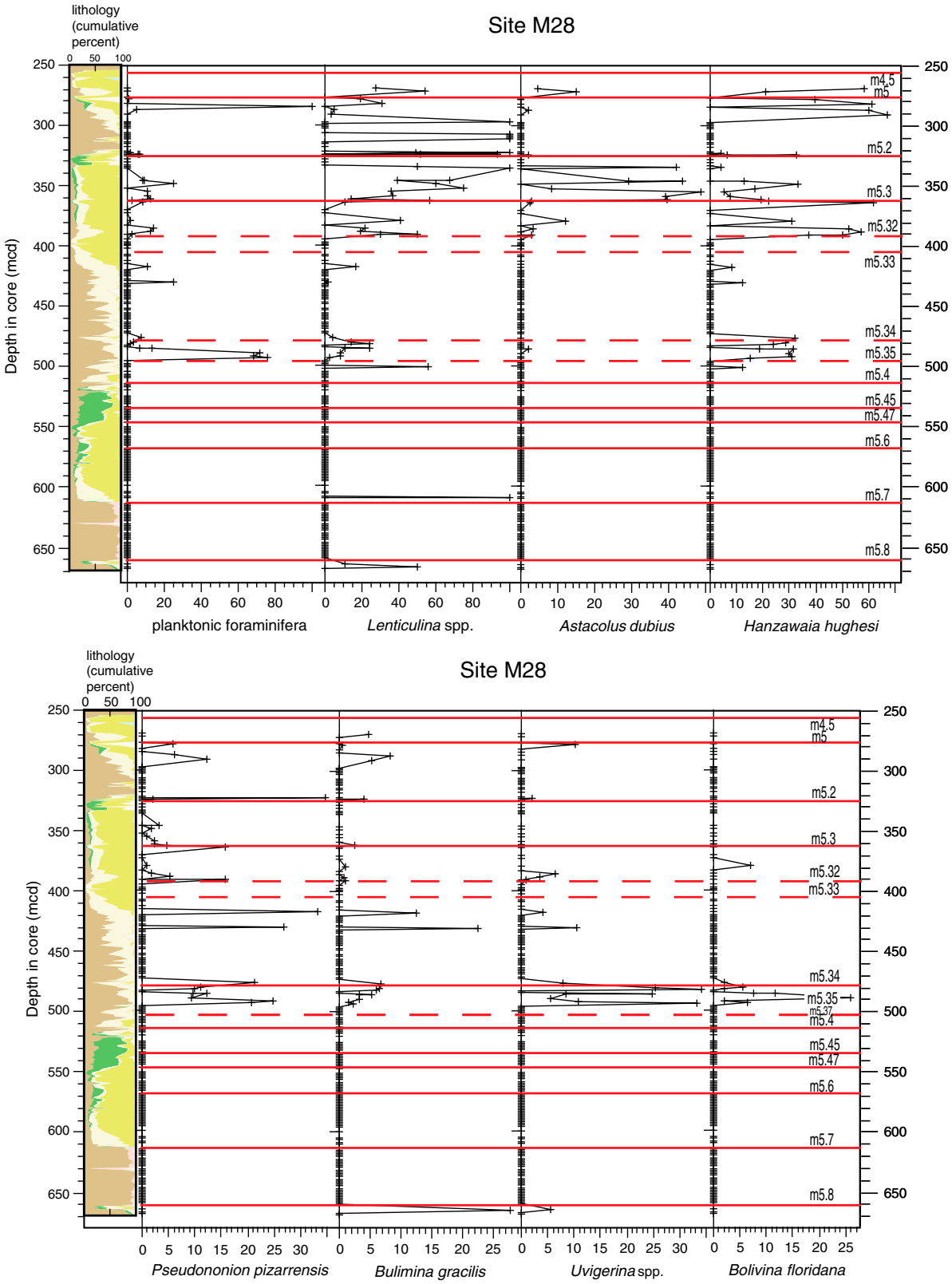

Figure 8. Integrated Ocean Drilling Program Expedition 313 Site M28 relative abundances (percentages) of dominant species delineated by factor analysis, along with percentage of planktonic foraminifera, shown within the sequence stratigraphic framework (mcd—meters composite depth). Samples examined for benthic foraminifera are indicated in the samples column. The cumulative percentage plot shows lithology (Miller et al., 2013a). Brown—mud; light yellow—fine quartz sand; dark yellow—medium-coarse quartz sand; green—glauconite sand; blue—carbonate (shells and foraminifera).

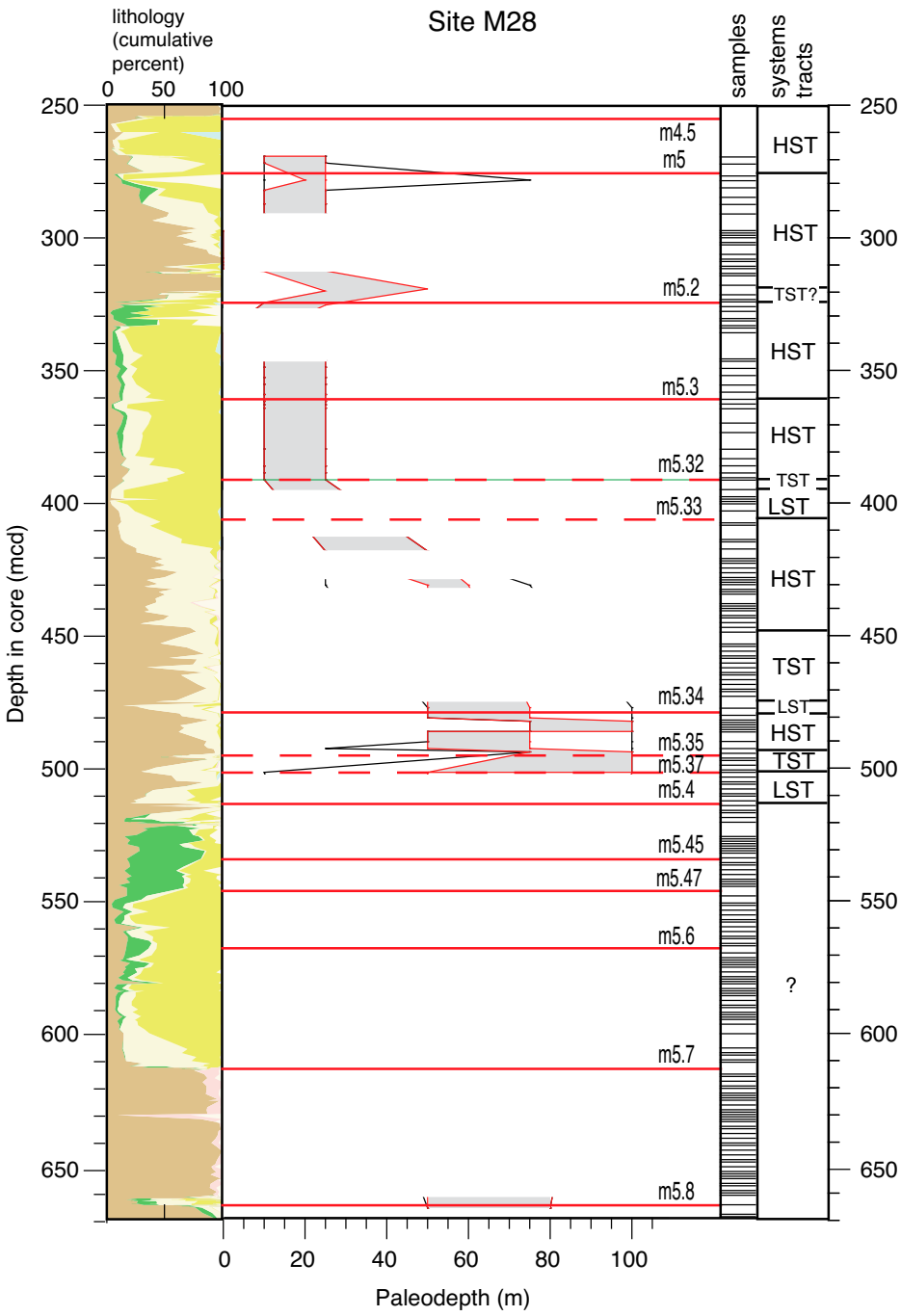

Figure 9. Integrated Ocean Drilling Program Expedition 313 Site M28 paleodepths are estimated from benthic foraminifera and shown within the sequence stratigraphic framework (mcd—meters composite depth). Shaded swath is best estimate; black envelope indicates possible paleodepth range. Systems tracts interpretations are shown. TST—transgressive systems tract; LST—lowstand systems tract; HST—highstand systems tract. The cumulative percentage plot shows lithology (Miller et al., 2013a). Brown—mud; light yellow—fine quartz sand; dark yellow—medium-coarse quartz sand; green—glauconite sand; blue—carbonate (shells and foraminifera).

variance explained by 5 factors (Fig. 10). Factor 1 accounts for 35.68% of the total variance and is characterized by *Uvigerina* spp. (*U. calvertensis*, *U. juncea*, *U. modeloensis*, and *U. subperegrina*; 75–100 m). Factor 2 (20.45% of the total variance) is characterized by *Lenticulina* spp. Factor 3 (11.53% of the total variance) is characterized by *B. gracilis* (50–80 m), *B. paula*, and *Hanzawaia* sp. 1. Factor 4 (9.57% of the total variance) is characterized by *H. hughesi* (10–25 m). Factor 5 (12.68% of the total variance) is characterized by *P. pizarrensis* (25–50 m).

Factor analysis indicates that there is an overall paleobathymetric shallowing upsection, with short-term variations superimposed on the long-term trend (Fig. 12). From ~750–490 mcd, paleodepths are ~75–100 m, and sometimes as deep as 120 m or as shallow as 25 m. From ~330 to 490 mcd, paleodepths are centered around 50–80 m, with variations from 10 to 100 m.

Within-Sequence Trends

Eocene Sequence

At Site M27, the only sample (630.17 mcd) examined from a fine-grained Eocene sequence (625.83 mcd to base of hole, 631.15 mcd) deposited in offshore environments (Mountain et al., 2010) is characterized by a diverse, deeper shelf benthic foraminiferal assemblage (e.g., *Alabamina midwayensis*, *C. pachyderma, Trifarina wilcoxensis*, *Siphonina*

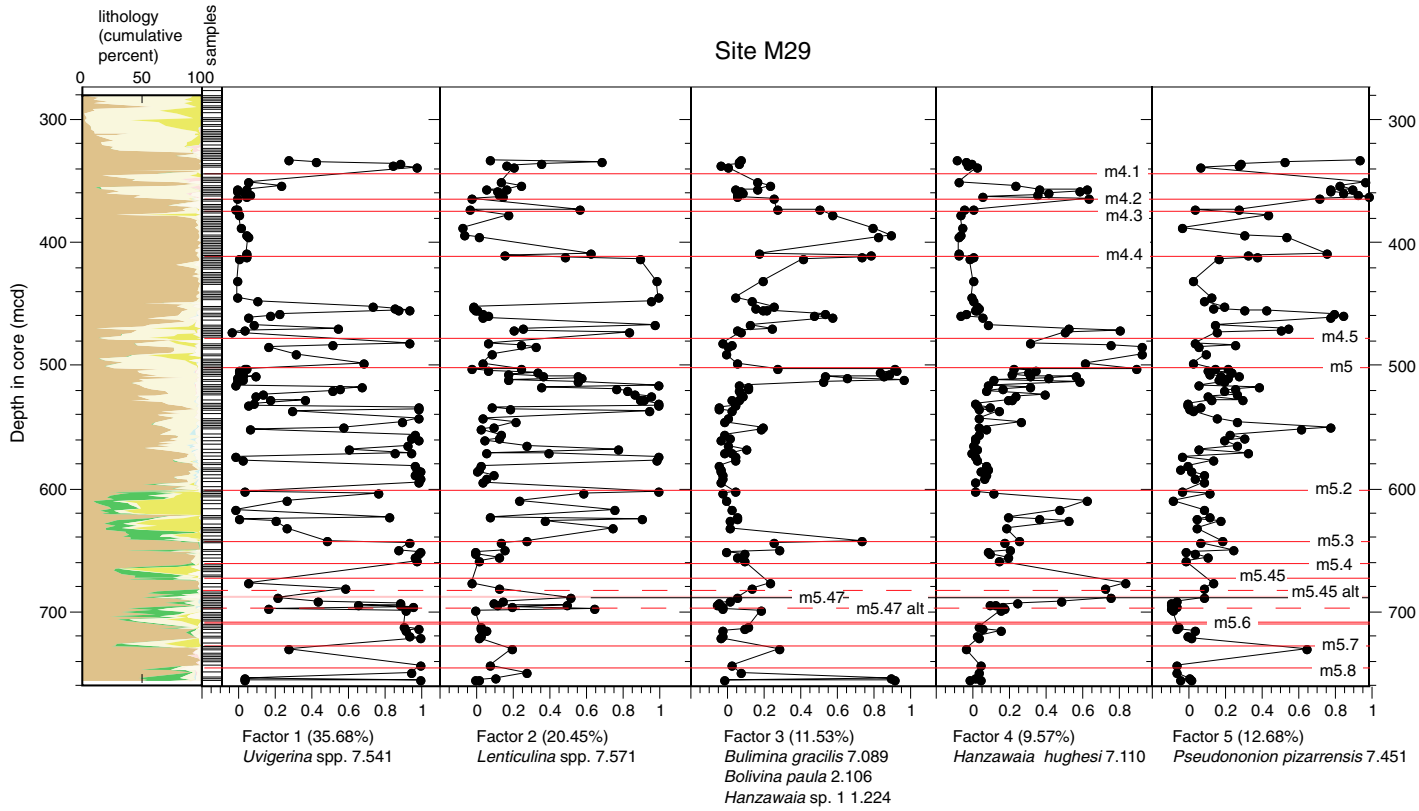

Figure 10. Integrated Ocean Drilling Program Expedition 313 Site M29 factors within the sequence stratigraphic framework (mcd—meters composite depth). Samples examined for benthic foraminifera are indicated in the samples column. Species that characterize each factor are shown with the factor scores, along with the variance explained by each factor. The cumulative percentage plot shows lithology (Miller et al., 2013a). Brown—mud; light yellow—fine quartz sand; dark yellow—medium-coarse quartz sand; green—glauconite sand; blue—carbonate (shells and foraminifera).

claibornensis) and abundant planktonic foraminifera (47.9%), indicating ~100–120 m paleodepth (Figs. 4–6).

Sequence O1

Sequence O1 was found only at Site M27 (625.83–617 mcd, ca. 32.3–32.2 Ma), where it consists of glauconitic clay. The sample (618.02 mcd) examined from this sequence is characterized by a diverse, deeper shelf benthic foraminiferal assemblage (e.g., *A. midwayensis*, *C. pachyderma*, *Hoeglundina elegans*, *S. claibornensis*, *Sphaeroidina bulloides*), indicating ~100–120 m paleodepth (Figs. 4–6).

Sequence O3

Sequence O3 was found only at Site M27 (617–538.68 mcd, 29.3–28.2 Ma), where it was deposited on a bottomset (Fig. 2). The lithology consists of a basal glauconitic-quartzose sandy clay, a glauconite clay, and glauconitic quartzose clay–clayey glauconitic quartz sand (Miller et al., 2013a). We examined 23 samples in this sequence. Benthic foraminiferal assemblages indicate variability within outer middle neritic depths (75–100 m) throughout this section (Figs. 4–6). Planktonic foraminiferal abundances are ~0%–2%; this is lower than expected for this water depth (Grimsdale and van Morkhoven, 1955), but there is no evidence of dissolution of the planktonic foraminifera in these samples. The dominance of the *Uvigerina* spp.–*Gyroidinoides* spp. biofacies (factor 5), together with the lack of *B. gracilis*, indicates paleodepths of 80–100 m from ~601.35 to 593.41 mcd (Figs. 4–6). Above this, an increase in taxa such as *C. pachyderma*, *Gyroidinoides* spp., and *Melonis pompilioides* indicates a slight deepening to 90–100 m (592.07–589.10 mcd). A slight deepening to ~100 m is indicated by a shift to the *C. primulus*–*Gyroidinoides* spp. biofacies (factor 4), and higher abundances of *C. pachyderma* in many samples (570.73–549.04 mcd). A shift back to the factor 5 *Uvigerina* spp.–*Gyroidinoides* spp. biofacies indicates 75–100 m paleodepth at the top of this sequence (543.30–540.21 mcd). The *Lenticulina* spp. biofacies (factor 2) occurs intermittently throughout the sequence. These paleodepth variations may indicate flooding surfaces associated with parasequence boundaries (Figs. 4–6).

Sequence O6

Uppermost Oligocene sequence O6 is found only at Site M27 (538.68 to 509 or 515 mcd; 23.5–23.0 Ma), where it is dominated by clayey, slightly glauconitic fine quartz sand. The entire sequence (11 samples examined) is characterized by the *Uvigerina* spp.–*Gyroidinoides* spp. biofacies (factor 5), indicating 75–100 m paleodepth from ~538.56 to 513.31 mcd (Figs. 4–6). Elevated abundances of *B. gracilis* and higher loadings on factor 1 at 531.09 mcd indicate a shallowing to the upper end of the depth range for this sample, to ~75–80 m paleodepth.

Sequence m6

Sequence m6 was fully recovered only at Site M27 (509/515–494.87 mcd, 20.9–20.7 Ma), where it consists of clayey glauconite-quartz sands deposited in a bottomset. Two samples

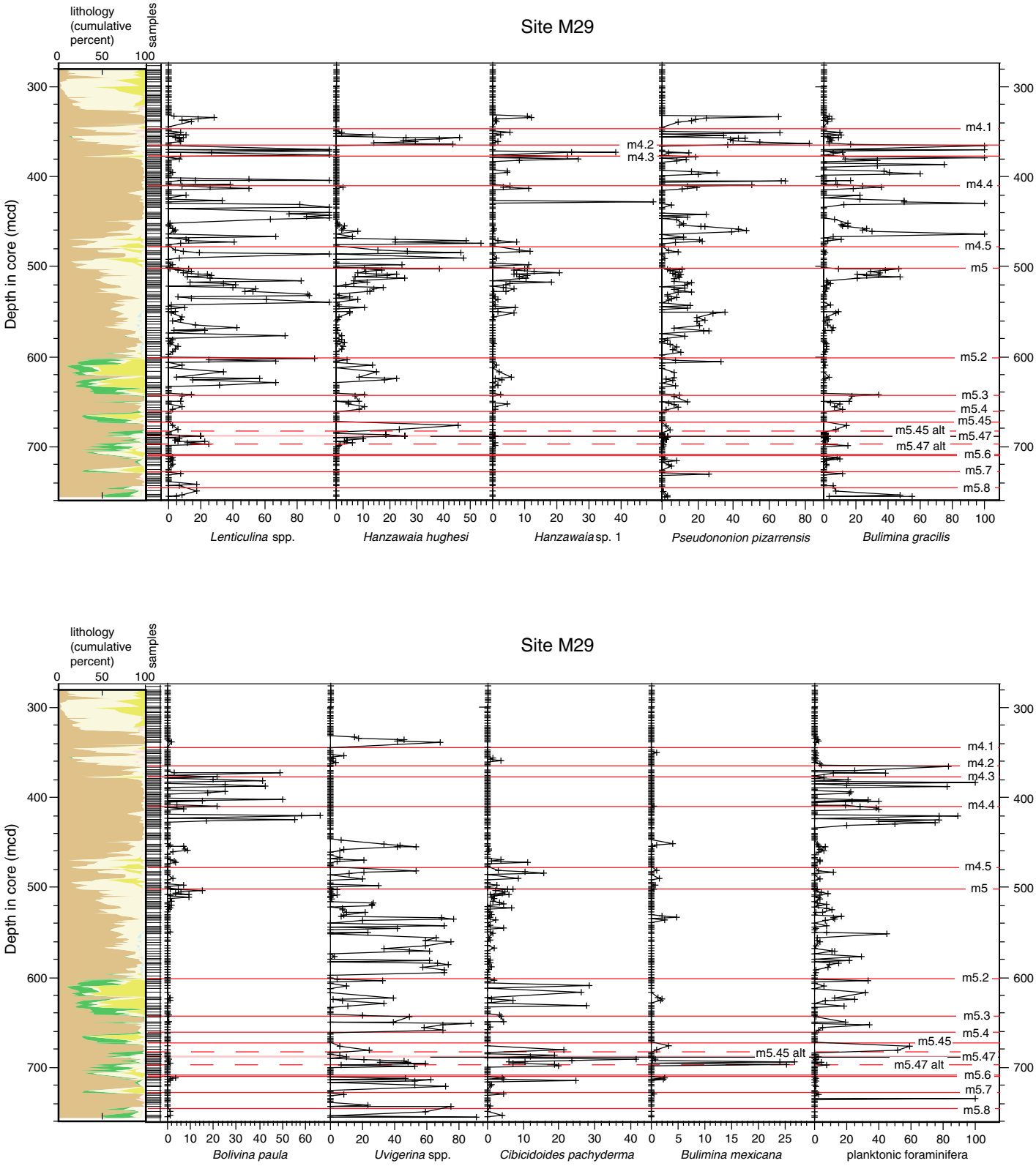

Figure 11. Integrated Ocean Drilling Program Expedition 313 Site M29, relative abundances (percentages) of dominant species delineated by factor analysis, along with percentage of planktonic foraminifera, shown within the sequence stratigraphic framework (mcd—meters composite depth). Samples examined for benthic foraminifera are indicated in the samples column. The cumulative percentage plot shows lithology (Miller et al., 2013a). Brown—mud; light yellow—fine quartz sand; dark yellow—medium-coarse quartz sand; green—glauconite sand; blue—carbonate (shells and foraminifera).

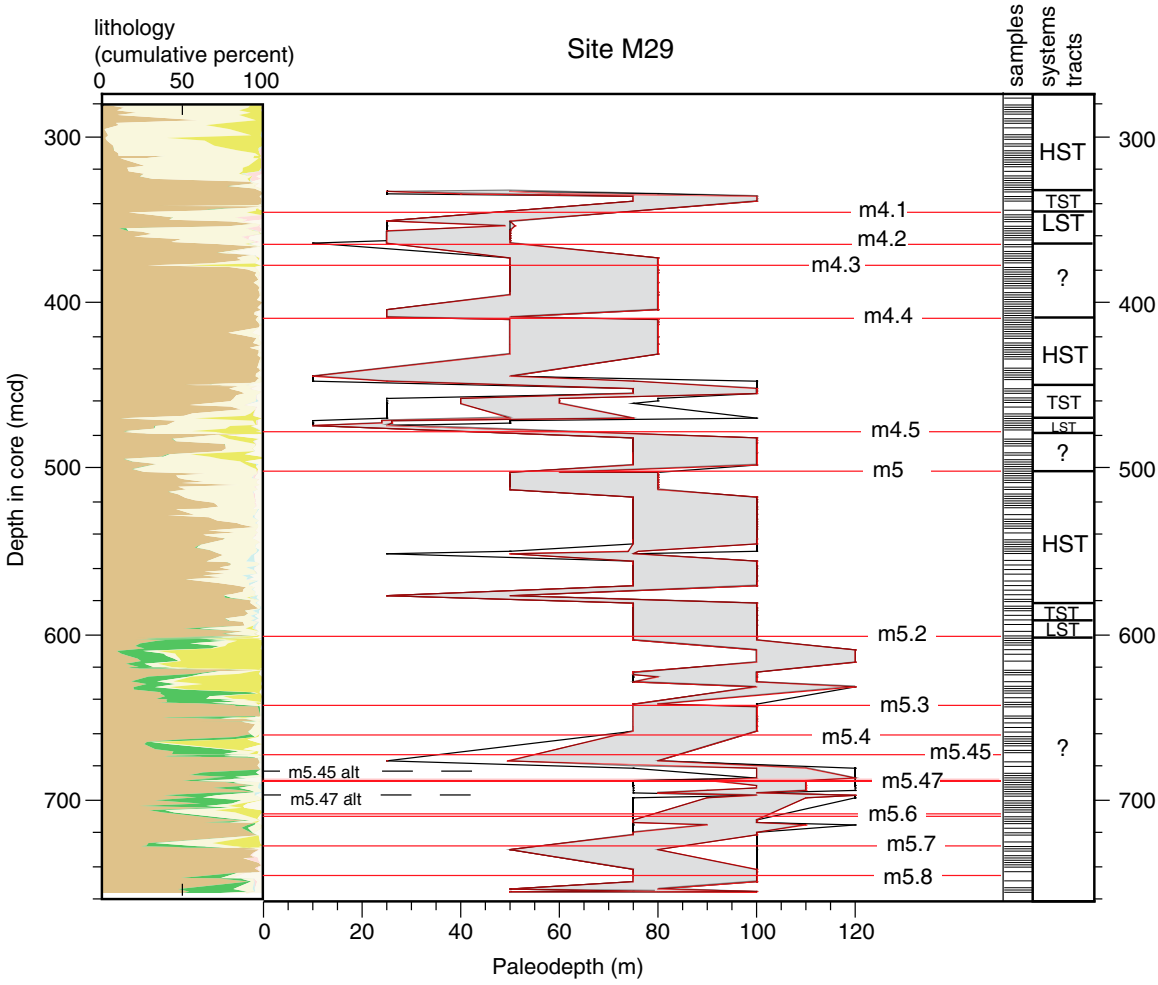

Figure 12. Integrated Ocean Drilling Program Expedition 313 Site M29 paleodepths are estimated from benthic foraminifera and shown within the sequence stratigraphic framework (mcd—meters composite depth). Shaded swath is best estimate; black envelope indicates possible paleodepth range. Systems tracts interpretations are shown. TST—transgressive systems tract; LST—lowstand systems tract; HST—highstand systems tract. The cumulative percentage plot shows lithology (Miller et al., 2013a). Brown—mud; light yellow—fine quartz sand; dark yellow—medium-coarse quartz sand; green—glauconite sand; blue—carbonate (shells and foraminifera).

yielded depth-diagnostic benthic foraminifera; most samples (5) were either barren or did not yield depth-diagnostic foraminifera. The lowermost sample (508.87 mcd) is characterized by the *Uvigerina* spp.–*Gyroidinoides* spp. fauna (factor 5), indicating ~75–100 m paleodepth (Figs. 4–6). A shallowing within the middle neritic zone from ~75–100 m water depth at the base of the sequence to 50–80 m paleodepth in the middle of the sequence (500.60 mcd) is indicated by an increase in *B. gracilis*.

At Site M28, the 3 samples examined in the partially recovered m6 sequence (below 662.98 mcd) yielded too few foraminifera to make a firm paleodepth estimate, although sparse benthic foraminifera at 664.22 mcd may indicate 50–80 m paleodepth, based on *B. gracilis* abundance.

Sequence m5.8

The foreset of sequence m5.8 was cored at Site M27 (494.87–361.28 mcd; 20.1–19.2 Ma) near where the sequence reaches its maximum thickness and appears stratigraphically most complete. We examined 61 samples for biofacies. Benthic foraminifera are absent from all 24 samples in the lower part of the sequence (494.77–469.895 mcd; Figs. 4–6 and 13). Two coarsening-upward successions in the lower part of the sequence (494.87–485; 485–477.52 mcd) were deposited on a bottomset and are interpreted as an LST (Miller et al., 2013b). The TS is placed at the change from regressive to transgressive sedimentary facies at 477.52 mcd, marking the top of the LST.

The LST is overlain by a fined-grained succession to ~415 mcd, deposited in a river-influenced offshore environment (Mountain et al., 2010) (Figs. 6 and 13). A fining-upward succession from 477.52 to 460 mcd indicates a deepening above the TS. A deeper water section (50–80 m paleodepth; 467.01–421.31 mcd) at Site M27 is indicated by the *B. gracilis* biofacies (factor 1). Within this section, variations in water depth are interpreted based on changing abundances of secondary taxa, with higher abundances of *P. pizarrensis* (factor 3) indicating shallowing to ~50–60 m, and higher abundances of *Uvigerina* spp. indicating deeper water (~75–80 m; Figs. 4–6 and 13). High loadings on both factor 1 (*B. gracilis*) and factor 5 (*Uvigerina* spp. and *Gyroidinoides* spp.), along with high planktonic foraminiferal abundances, indicate 75–80 m paleodepth in two samples (463.865, 460.96 mcd). The paleodepth

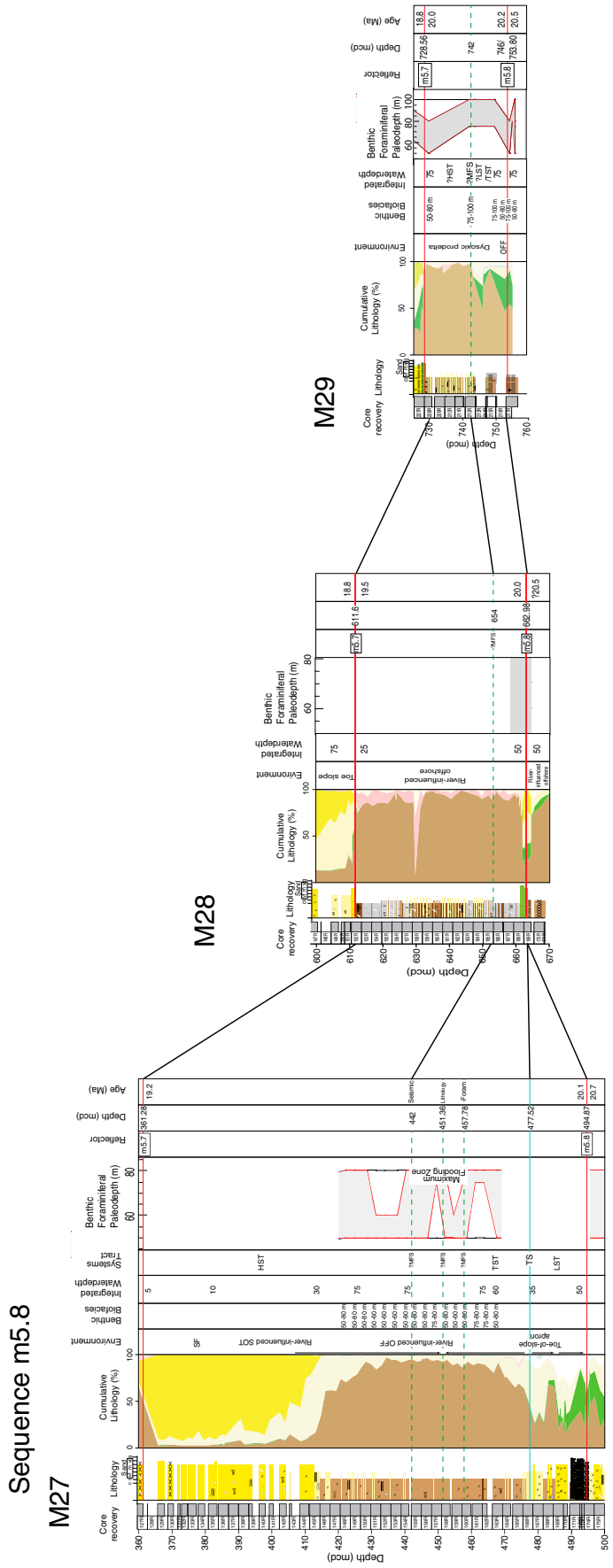

Figure 13. Sequence m5.8 comparisons among Integrated Ocean Drilling Program Expedition 313 Sites M27, M28, and M29 showing detailed paleobathymetry and systems tracts based on foraminiferal and lithologic interpretations. Core depths are in meters composite depth (mcd); also shown are core number (R—rotary), and core recovery (gray—recovered, white—gap). Components of figure that are taken from Miller et al. (2013b): cumulative lithology (brown—mud; light yellow—fine quartz sand; dark yellow—medium-coarse quartz sand; green—glauconite sand; blue—carbonate [shells and foraminifera]; pink—mica), lithology (after Mountain et al., 2010; c—clay; s—silt; vf—very fine sand; m—medium sand; vc—very coarse sand; g—gravel and/or pebbles), environmental interpretation based in lithofacies (SF—shoreface; SOT—shoreface-offshore transition; LS—lower shoreface; OFF—offshore), integrated water depth in meters based on benthic foraminiferal biofacies and lithofacies, reflectors (horizontal lines: red—sequence boundary, blue—transgressive surface [TS], green—maximum flooding surface [MFS]), and depths to reflectors. TST—transgressive systems tract; LST—lowstand systems tract; HST—highstand systems tract.

fluctuations in this section are also evident in palynomorph distance from shoreline estimates (McCarthy et al., 2013), and may indicate flooding surfaces associated with parasequence boundaries.

Peak planktonic abundances at 457.78 mcd suggest that this may be the MFS. Another peak in the *B. gracilis* and *Uvigerina* spp.–*Gyroidinoides* spp. biofacies (factors 1 and 5) at ~448.42 mcd may be an FS, although benthic foraminiferal abundances are low in this sample. Uniform, very slightly sandy, silty clay from 460 to 440 mcd does not contain a single discrete surface that can be identified as the MFS. Lithologic criteria suggest that the MFS occurs at 451.36 mcd or 448 mcd where mica, laminations, and percent sand reach a minimum (Fig. 13). A major downlap surface appears to tie to 442 mcd at Site M27 and is the best seismic candidate for an MFS. The slight differences in placement based on seismic, lithologic, and benthic foraminiferal criteria illustrate that picking an unequivocal MFS is complicated. Therefore, we conclude that instead of a distinct MFS, there is a zone of maximum flooding from 460 to 440 mcd (see Loutit et al., 1988).

Offshore silts continue to characterize the sediments up to ~435 mcd. Above this, fine sands deposited in shoreface-offshore transition environments are overlain by medium- to coarse-grained sands deposited in shoreface environments. The transition to the sand-dominated lithofacies that begins at ~435 mcd suggests that the section above this is part of the HST. Samples in most of the HST are barren (above 420 mcd; Figs. 4–6).

At Site M28, there were no benthic foraminifera in 37 samples examined from sequence m5.8 (662.98–611.60 mcd; 20–19.5 Ma; Figs. 7–9 and 13).

In sequence m5.8 at Site M29 (753.80/746–728.56 mcd; 20.2–20 Ma), 14 samples were examined for biofacies. The lowermost samples are dominated by the *Uvigerina* spp. biofacies (factor 1) that indicates paleodepths of 75–100 m, or by the *B. gracilis–B. paula–Hanzawaia* sp. 1 biofacies (factor 2) that indicates paleodepths of 50–80 m (Figs. 10–13). This is overlain by barren samples. A single sample near the top of sequence m5.8 is characterized by the factor 2 biofacies, indicating 50–80 m paleodepths.

Paleodepths indicated by the biofacies in sequence m5.8 are 50–80 m in a foreset at Site M27, with 50–60 m or 75–80 m indicated in some samples (Figs. 6 and 13). Situated in a prodelta bottomset at Site M29, biofacies indicate overall deeper paleodepths, ranging from 50–80 m to 75–100 m (Figs. 12 and 13).

Sequence m5.7

At Site M27, seismic profiles show the thin (5.75 m) sequence m5.7 (361.28–355.53 mcd) as a remnant immediately landward of the rollover (Fig. 2). No foraminifera were found in the two samples examined in this sequence, consistent with the interpretation of shallow-water (shoreface) deposits (Mountain et al., 2010) (Figs. 4–6 and 14). The sequence coarsens upsection, likely reflecting an HST. At Site M28, sequence m5.7 (611.6–567.5 mcd; 18.8–18.6 Ma) coarsens upsection to uniform medium sands (~595 mcd) devoid of foraminifera (32 samples examined), deposited on a bottomset (Figs. 4–6 and 14). Sequence m5.7 at Site M29 (728.56 to 710 or 707.56 mcd; ca. 18.8–18.6 Ma) is a basal glauconitic quartz sand that fines upward to a fine to coarse sand, and then to an offshore clay, all deposited on a bottomset. We examined 11 samples in this sequence. The lowermost 3 samples are barren (728.46–726.16 mcd). Above this, the *Uvigerina* spp. biofacies (factor 1) indicates paleodepths of 75–100 m in this sequence (721.08–712.31 mcd). A dramatic increase in the abundance of *C. pachyderma* at 714.94 mcd indicates a deeper paleodepth (90–110 m; Figs. 10–12 and 14).

Sequence m5.6

Sequence m5.6 is absent from Site M27. At Site M28, sequence m5.6 (567.5–545.5 mcd) is a bottomset sand devoid of foraminifera (13 samples examined). At Site M29, sequence m5.6 (710 or 707.56 to 695.65 or 687.87 mcd; 18.3–18.1 Ma; 11–17 samples examined) is barren in the lower section (710–700.08 mcd; Figs. 10–12). Benthic foraminiferal biofacies from 698.58 to 686.54 mcd (which encompasses the uncertain zone of the sequence m6-m5.47 transition) indicate that the entire section was deposited in relatively deep water (75–120 m), likely with fluctuations within this paleodepth range (Figs. 10–12). Two samples (698.58, 697.07 mcd) within sequence m5.6 have high loadings on the factor 1 biofacies (*Uvigerina* spp.), indicating paleodepths of 75–100 m. However, deeper paleodepths are indicated by high abundances of *C. pachyderma* (~20%) in both samples, coupled with the disappearance of shallower water taxa (*B. gracilis*) especially in the upper sample; therefore, we place 698.58 mcd at 90–110 m paleodepth, and 697.10 mcd at 100–120 m paleodepth (Figs. 10–12). Similarly, the *Uvigerina* spp. biofacies (factor 1), low abundances of *B. gracilis*, and moderate to high abundances of *C. pachyderma* (~6%–42%) in all samples from 695.60 to 686.54 mcd indicate paleodepths ranging from 80 to 100 m to 100–120 m within this section.

Sequence m5.47

At Site M27, sequence m5.47 (355.53–336.06 mcd) consists of glauconitic sands that are interpreted as channel-fill deposits and that cannot be dated (Mountain et al., 2010). It is devoid of foraminifera (5 samples examined). At Site M28, this sequence (545.5–533.59 mcd) consists of glauconite-quartz sands deposited on a bottomset that is devoid of foraminifera (10 samples examined).

At Site M29, both the upper and lower boundaries that mark sequence m5.47 are uncertain (695.65 or 687.87 to 681 or 673.81 mcd; 18.0–17.9 Ma; 6–13 samples examined). Samples from 683.46, 684.81, and 685.75 mcd are barren. The top of sequence m5.47 may be at 681 or 673.81 mcd. Two samples within this interval yield benthic foraminifera (680.32 and 677.29 mcd). For 680.32 mcd, the *Uvigerina* spp. biofacies (factor 1) and ~21% *C. pachyderma* indicate a paleodepth of ~90–110 m, with a downslope transport component indicated by ~23% *H. hughesi*. Similarly, the sample at 677.29 mcd is characterized by factor 4 (*Hanzawaia* biofacies with ~46% *H. hughesi*) and contains common *B. gracilis* (~14%) and *Uvigerina* spp. (~6%), indicating 25–80 m paleodepth with possible downslope transport; based on the species abundances and ~59% planktonic foraminifera, we narrow this estimate to 50–80 m paleodepth with downslope transport (Figs. 10–12).

Sequence m5.45

At Site M27, sequence m5.45 (336.06–295.01 mcd; 18.0–17.7 Ma; 28 samples examined) shows two distinct coarsening-upward parasequences (336–323 and 323–309 mcd) within an otherwise fine-grained unit (Miller et al., 2013a). The lowermost two samples (335.85 and 332.79 mcd) are barren (Figs. 4–6), and may be either LST or transported sediments within a TST (as interpreted in Miller et al., 2013a). The factor 3 biofacies (*P. pizarrensis*, *Hanzawaia* sp. 1, and *H. hughesi*) indicates paleowater depths of ~25–50 m for 329.81 mcd and 318.81–311.46 mcd; based on moderate abundances of *B. gracilis* and *Uvigerina* spp., and abundant planktonic foraminifera (~7%–43%), we narrow this paleodepth estimate to 40–50 m for most of the section, possibly shallowing to 25–50 m toward the top. We tentatively place the MFS at the highest peak in planktonic foraminifera (~43%) and a secondary mud peak (329.81 mcd). A sample at the upper sequence boundary (295.01 mcd) has an estimated paleodepth of ~25 m paleodepth (Figs. 4–6 and 15). The shallowing indicated by the biofacies, overlain by barren samples, is consistent with the upper part of the sequence interpreted as an HST.

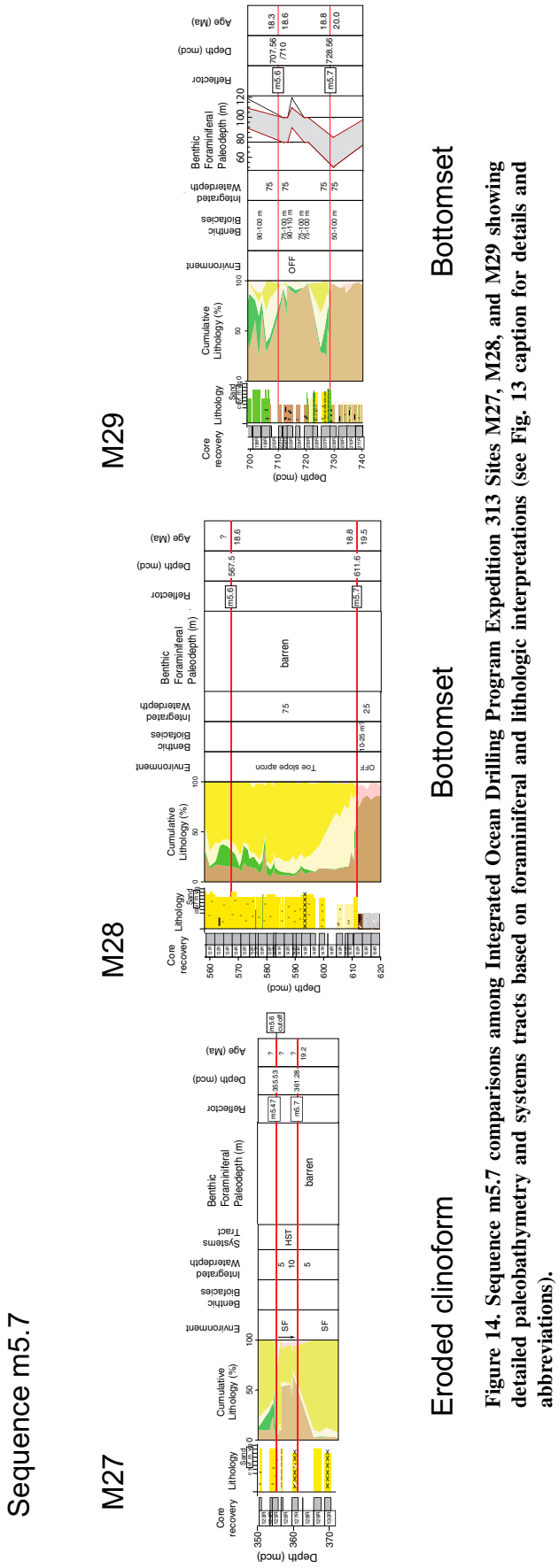

Figure 14. Sequence m5.7 comparisons among Integrated Ocean Drilling Program Expedition 313 Sites M27, M28, and M29 showing detailed paleobathymetry and systems tracts based on foraminiferal and lithologic interpretations (see Fig. 13 caption for details and abbreviations).

At Sites M28 and M29, samples from sequence m5.45, deposited as bottomsets, were devoid of foraminifera (13 samples examined at Site M28; 10 samples examined at Site M29).

Sequence m5.4

Analysis of seismic profiles, core data, and log stacking patterns of the section between sequence m5.4 and m5.3 reflectors led to the conclusion (Miller et al., 2013b) that sequence m5.4 is actually a composite of three higher order (100 to 400 k.y. scale) sequences called m5.4–1 (the sequence that directly overlies surface m5.4), m5.34, and m5.33. All three sequences are found at Site M28, which was drilled through the foreset. At Site M27, sequences m5.34 and m5.33 are found at the topset, but sequence m5.4–1 apparently is eroded. At Site M29, drilled on a bottomset, the seismic resolution did not permit the higher order sequences to be defined and the section there is referred to as m5.4 (Miller et al., 2013b).

At Site M27, sequence m5.34 (295.01–271.23 mcd; 17.0–16.9 Ma; 19 samples examined) was deposited on a topset (Figs. 2 and 16). A sample (295.01 mcd) at the base of sequence m5.34 contains ~29% *H. hughesi*, ~17% *P. pizarrensis*, and ~51% *Lenticulina* spp., indicating ~25 m paleodepth. Samples at 294.71 and 294.12 mcd are characterized by the *P. pizarrensis* biofacies (factor 3), indicating ~25–50 m water depth; we narrow this depth estimate to 40–50 m, based on ~14%–15% *Uvigerina* spp. in these two samples, and place it within the TST (Figs. 4–6 and 16). Barren samples extend from 293.18 up to 268.84 mcd, consistent with HST deposition (Miller et al., 2013b).

The m5.33 sequence at Site M27 (271.23–256.19 mcd; 16.9–16.8 Ma; 13 samples examined) was deposited on a topset. Barren samples are interspersed with occasional samples (265.74, 264.56, 261.09 mcd) that yield the *P. pizarrensis* biofacies (factor 3), indicating ~25–50 m paleodepth (Figs. 4–6 and 16). One of these samples (264.56 mcd) also has ~14% *Uvigerina* spp., indicating a paleodepth at the deep end of this range (35–50 m). Facies trends above m5.33 are unclear, but the ~35–50 m paleodepth at 264.56 mcd is consistent with a major downlap surface (263 mcd) identified in Miller et al. (2013b) as the MFS. The overlying HST (9 samples examined) is mostly devoid of foraminifera, with the exception of 261.09 mcd, which is characterized by the *P. pizarrensis* biofacies (factor 3), indicating ~25–50 m (Figs. 6 and 16).

Site M28 cored composite sequence m5.4 (512.33–361 mcd; 17.7–16.6 Ma; 80 samples examined) on the foreset where the sequence

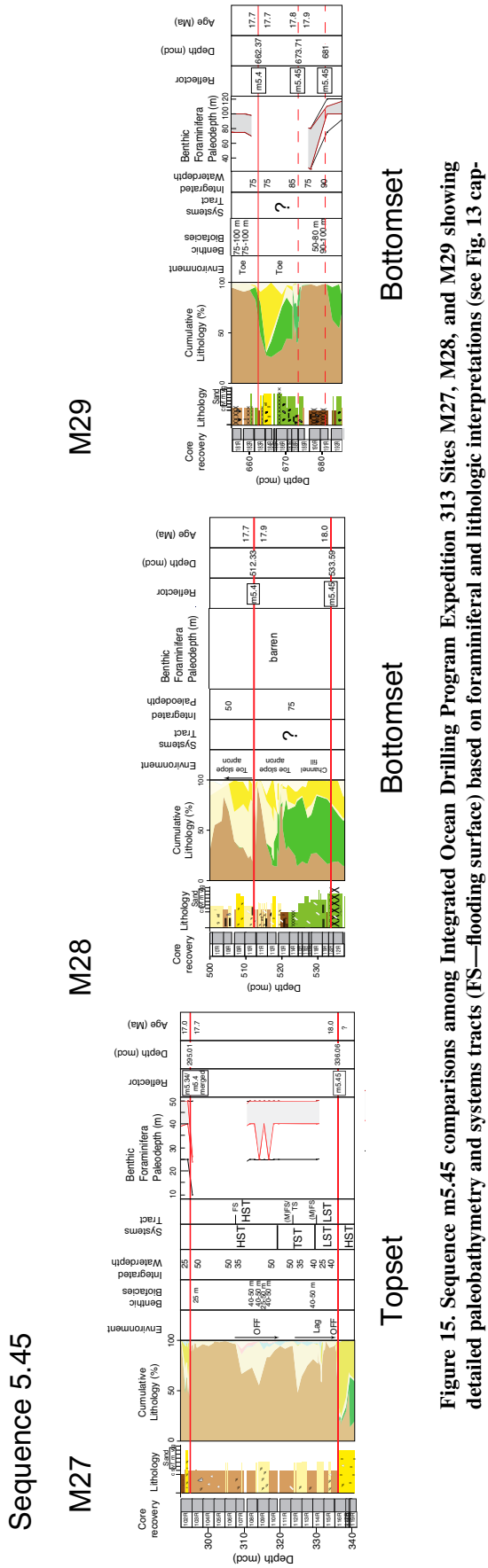

Figure 15. Sequence m5.45 comparisons among Integrated Ocean Drilling Program Expedition 313 Sites M27, M28, and M29 showing detailed paleobathymetry and systems tracts (FS—flooding surface) based on foraminiferal and lithologic interpretations (see Fig. 13 caption for details and abbreviations).

is thickest (Figs. 2, 7–9, and 16). Higher order sequences m5.4–1 (512.33 mcd), m5.34 (479 mcd), and m5.33 (405 mcd) were identified in Miller et al. (2013b) based on seismic, core, and stacking patterns. Within sequence m5.4–1 (512.33–479 mcd), barren samples characterize the LST, with sparse benthic foraminifera marking the TS at ~501 mcd at the beginning of a fining-upward section (Figs. 7–9 and 16).

An intrasequence reflection (m5.35, 494 mcd) at Site M28 corresponds to the contact between a thin sand bed over a clayey silt, which coincides with a transition to foraminiferal assemblages (factor 3, *Uvigerina* spp. and *B. floridana*; factor 5, *P. pizarrensis* and *B. gracilis*; factor 1, *H. hughesi*; factor 2, *Lenticulina* spp.) that indicate ~50–100 m paleodepth (493.77–485.335 mcd). We interpret this contact as the MFS, with the HST above. Variability of species abundances and factor-defined biofacies within this interval (493.77–485.335 mcd) indicate paleodepth fluctuations, with higher abundances of *Uvigerina* spp. (493.77, 485.335 mcd) indicating 75–100 m, and higher abundances of *H. hughesi* and *P. pizarrensis* (492.26, 489.20, 486.17 mcd) indicating 50–75 m paleodepth (Figs. 7–9 and 16). Abundant planktonic foraminifera (to 76%) support the deep-water setting indicated by the biofacies in this section. These samples are in the lower portion of a coarsening-upward, regressive package from m5.35 (494 mcd) to m5.34 (479 mcd), associated with shoreface-offshore transition and offshore deposits. The middle portion yields barren samples (484.37–482.5 mcd). The upper portion (481.4–477.07 mcd) is characterized by the factor 3 biofacies (*Uvigerina* spp. and *B. floridana*) that indicates ~75–100 paleodepth; an upsection decrease in *Uvigerina* spp. and increases in *H. hughesi* and *P. pizarrensis* indicates somewhat shallower depths in the upper samples (50–75 paleodepth), consistent with the upsection lithologic coarsening (Figs. 7–9 and 16) and interpretation of the section from 494 to 479 as an HST.

Reflector m5.34 (479 mcd) is interpreted as a sequence boundary. Coarsening (479–475 mcd) and fining (475–449 mcd) upward successions are interpreted as an LST and a TST, respectively, but are devoid of foraminifera. A coarsening-upward, regressive HST package (449–415 mcd) is associated with a shift from offshore to shoreface-offshore transition deposits. Samples in this section are barren up through 395.12 mcd, with 2 exceptions. The *P. pizarrensis–B. gracilis* biofacies (factor 5) indicates 25–80 m paleodepth, which we refine based on abundances of shallow versus deep secondary taxa, at 430.99 mcd (50–60 m paleodepth) and 417.13 mcd (25–50 m paleodepth; Figs. 7–9 and

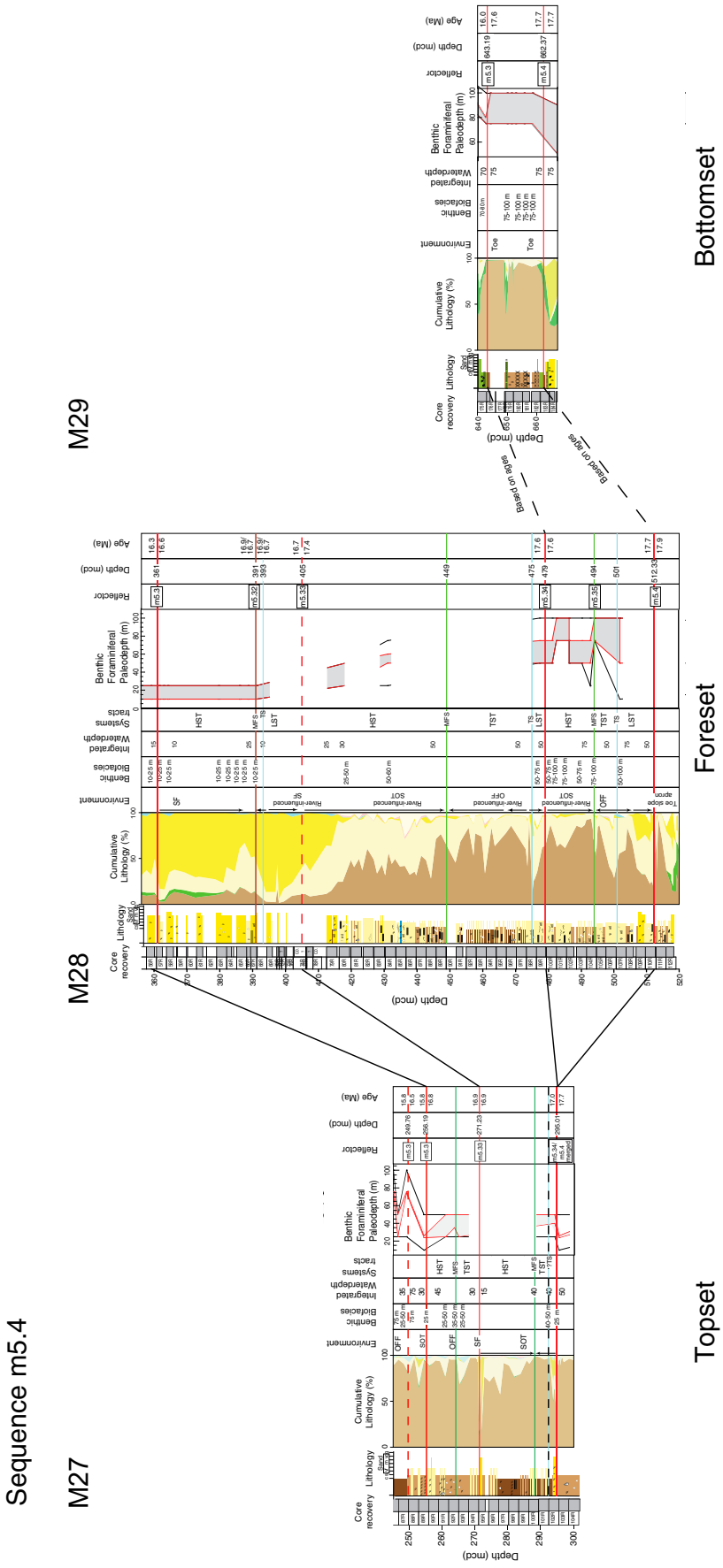

Figure 16. Sequence m5.4 comparisons among Integrated Ocean Drilling Program Expedition 313 Sites M27, M28, and M29 showing detailed paleobathymetry and systems tracts based on foraminiferal and lithologic interpretations (see Fig. 13 caption for details and abbreviations).

16). This supports the shallowing-upward interpretation derived from lithofacies.

Reflector m5.33 (405 mcd) tentatively is interpreted as a sequence boundary, whereas reflector m5.32 (391 mcd) is a major downlap surface that is an MFS overlain by an HST (m5.32-m5.3; 391–361 mcd). Samples from 391.2 to 361 mcd contain the *H. hughesi* biofacies (factor 1), indicating 10–25 m paleodepth. Samples straddling reflector m5.32 (389 mcd) contain common *Uvigerina* spp. and planktonic foraminifera (Fig. 8), consistent with this being an MFS and regressive HST above.

At Site M29, sequence m5.4 (662.37–643.19 mcd; 17.7–17.6 Ma; 8 samples examined) consists primarily of silt with floating granules and coarse quartz sand deposited on a bottomset and dated at this site with no discernible gap at its base. The entire sequence is characterized by outer middle neritic (75–100 m) foraminiferal assemblages, characterized by the *Uvigerina* spp. biofacies (factor 1; Figs. 10–12 and 16). No obvious water depth trends are discernible.

Sequence m5.3

The placement of the basal sequence boundary of m5.3 is equivocal at Site M27, either at 256.19 or 249.76 mcd (Miller et al. 2013a); we follow the level favored in Miller et al. (2013a), with m5.3 at 256.19 mcd based on the lithofacies. Sequence m5.3 (256.19–236.15 mcd; 15.8–15.6 Ma; 13 samples examined) was drilled on a topset consisting of either one or two fining-upward successions (depending on placement of the sequence boundary). The lowest sample examined in this sequence (255.06 mcd), within the first fining-upward succession, has high abundances of *P. pizarrensis*, *H. hughesi*, and *Hanzawaia* sp. 1, indicating ~25 m paleodepth (Figs. 5, 6, and 17). An upsection increase in abundance of *Uvigerina* spp. indicates ~75 m paleodepth in 2 samples (250.46 and 245.88 mcd), consistent with ~39% planktonic foraminifera; an intervening sample dominated by *Lenticulina* spp. (~73%) may contain transported shallow-water specimens. We interpret this as a TST with an MFS near the top of the sequence (Figs. 6 and 17).

At Site M28, sequence m5.3 (361–323.23 mcd; 16.3–15.7 Ma; 12 samples examined) was recovered immediately landward of the foreset (Fig. 2). This sequence consists of a thick pile of coarse slightly glauconitic quartz sand deposited in shoreface environments and capped by a channel (Fig. 17). Foraminiferal assemblages are dominated by *Lenticulina* spp. and *A. dubius* (Factors 2 and 4), which are not useful depth indicators (Fig. 7). Based on abundance of *H. hughesi*, we interpret paleodepths of 10–25 m for 358.37–346.26 mcd and a single

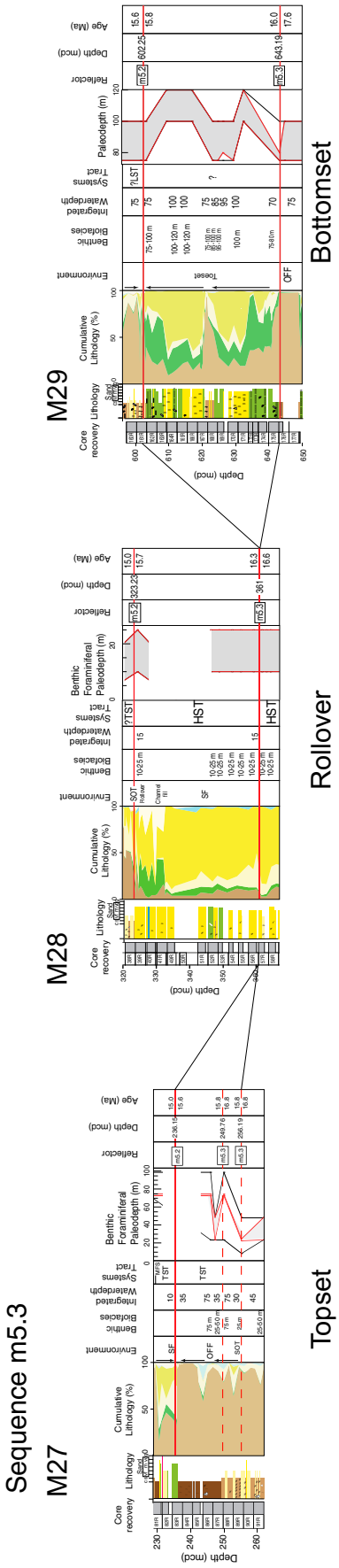

Figure 17. Sequence m5.3 comparisons among Integrated Ocean Drilling Program Expedition 313 Sites M27, M28, and M29 showing detailed paleobathymetry and systems tracts based on foraminiferal and lithologic interpretations (see Fig. 13 caption for details and abbreviations).

sample at 324.42 mcd (Figs. 7–9 and 17). Two samples (345.81 and 336.07 mcd) with few foraminifera, dominated by *Lenticulina* spp., may indicate dissolution, winnowing, and/or downslope transport. The shallow-water biofacies and barren samples are consistent with deposition in shallow water for this sequence.

At Site M29, sequence m5.3 (643.19–602.25 mcd; 16.0–15.8 Ma) was deposited on a bottomset with two coarsening-upward successions separated by a silt unit. Despite the abundant coarse sands in this sequence, benthic foraminifera indicate relatively deep water throughout, based on 19 samples examined. We note common specimens of transported *Lenticulina* spp. and *H. hughesi* along with deep-water taxa. We interpret this as an excellent example of transported shallow-water material mixed with in situ deep-water biofacies on a bottomset. The lowermost sample examined in this sequence (642.29 mcd) contains abundant *B. gracilis* (34%) and *Uvigerina* spp. (20%), indicating 75–80 m paleodepth (Figs. 10–11 and 17). Above this, samples through 633.13 mcd are barren. From 631.61 to 602.62 mcd, assemblages indicate water depth variations ranging from ~75 to 120 m. Samples with abundant *Uvigerina* spp. indicate deposition in the shallower depth of this range, whereas samples with more abundant *C. pachyderma* are interpreted to be deeper, 100–120 m paleodepth (631.61, 616.36, 610.26 mcd).

Portions of the TST and HST were preserved in the topset of sequence m5.3 at Site M27, with sparse foraminifera indicating paleodepths ranging from 25 to 75 m (Fig. 17). At Site M28, the shallower (0–25 m) HST sediments are preserved. Paleodepths in the bottomset at Site M29 vary from 75–100 m to 100–120 m, consistent with the deeper bottomset environment expected for the seismic geometry (Figs. 2 and 17).

Sequence m5.2

At Site M27, 3 samples were examined from sequence m5.2 (236.15–225.45 mcd; 15.0–14.8 Ma; Figs. 4–6), which was deposited on a topset (Fig. 2). The lower 2 samples were barren (233.14 and 232.19 mcd). A sample near the top of the sequence (227.27 mcd) yielded an assemblage dominated by *Lenticulina* spp. (58%); a paleodepth estimate of 75 m is inferred from 21% *Uvigerina* spp., together with very few shallow-water indicators (Figs. 4–6). We interpret the *Lenticulina* spp. as transported. We interpret the upsection facies change from a basal quartz sand to a medial clay yielding deeper water foraminifera (~75 m paleodepth) to an upper quartz sand as reflecting a thin TST, MFS, and thin truncated HST (Figs. 6 and 18).

Sequence m5.2 at Site M28 (323.23–276.81 mcd; 15.1–14.8 Ma; 21 samples examined) was drilled immediately landward of the foreset. Barren samples (321.38–313.41, 306.16–298.92, 297.07, 276.75 mcd) interspersed with shallow-water assemblages (10–25 m) characterize sequence m5.2 (Figs. 7–9 and 18). Samples with 100% *Lenticulina* spp. (312.06–307.71, 297.88 mcd) may indicate dissolution, winnowing, and/or downslope transport. Samples characterized by the *H. hughesi* biofacies (factor 1) indicate 10–25 m paleodepth (290.83, 287.40, 281.62, 278.64 mcd) at the top of the sequence. We use a qualitative assessment of the fine fraction (63–150 µm) to tentatively estimate paleodepths in several samples. (1) At 319.46 mcd, *P. pizarrensis*, *Uvigerina* spp., *H. hughesi*, and *Lenticulina* spp. possibly indicate ~50 m paleodepth, and (2) at 313.72 mcd, *H. hughesi*, *Lenticulina* spp., and planktonic foraminifera possibly indicate 10–25 m paleodepth. We place the MFS at a distinct burrowed surface at 320.55 mcd near a sample with the deepest biofacies at 319.72 mcd. The coarsening-upward sediments above ~310 mcd indicate shallowing upsection from offshore to shoreface-offshore transition to channel fill, indicating HST sediments. The barren samples interspersed with shallow-water assemblages (10–25 m) support this interpretation.

Site M29 sampled sequence m5.2 (602.25–502.01 mcd; 15.6–14.6 Ma; 50 samples examined) on a foreset just seaward of its maximum thickness, with the facies consisting primarily of fine sandy silt. The *Uvigerina* spp. biofacies (factor 1) characterizes much of this sequence (594.94–517.47 mcd) and indicates 75–100 m paleodepth; sporadic barren samples or samples with shallow-water species likely indicate downslope transport (Figs. 10–12 and 17). Two barren samples in the lowest part of the sequence occur in a coarsening-upward package (602–593 mcd) that is tentatively interpreted as the LST. The MFS is placed at peaks in planktonic foraminifera and mud at ~582 mcd. The section above this coarsens upward in general, and is interpreted as an HST with four parasequences bounded by FSs. A decrease in *Uvigerina* spp. abundances coupled with an increase in the factor 3 biofacies (*B. gracilis*, *B. paula*, and *Hanzawaia* sp. 1) in the upper part of the sequence (512.83–501.73 mcd) indicates somewhat shallower paleodepths within the middle neritic zone (50–80 m).

The biofacies in the topset of sequence m5.2 at Site M27 indicate 75–80 paleodepth in the TST and lower HST (Fig. 18). If the TST interpretation is correct and the recovered sections are coeval, then the shallower paleodepths (25–50 m) at Site M28 are unexpectedly shallow.

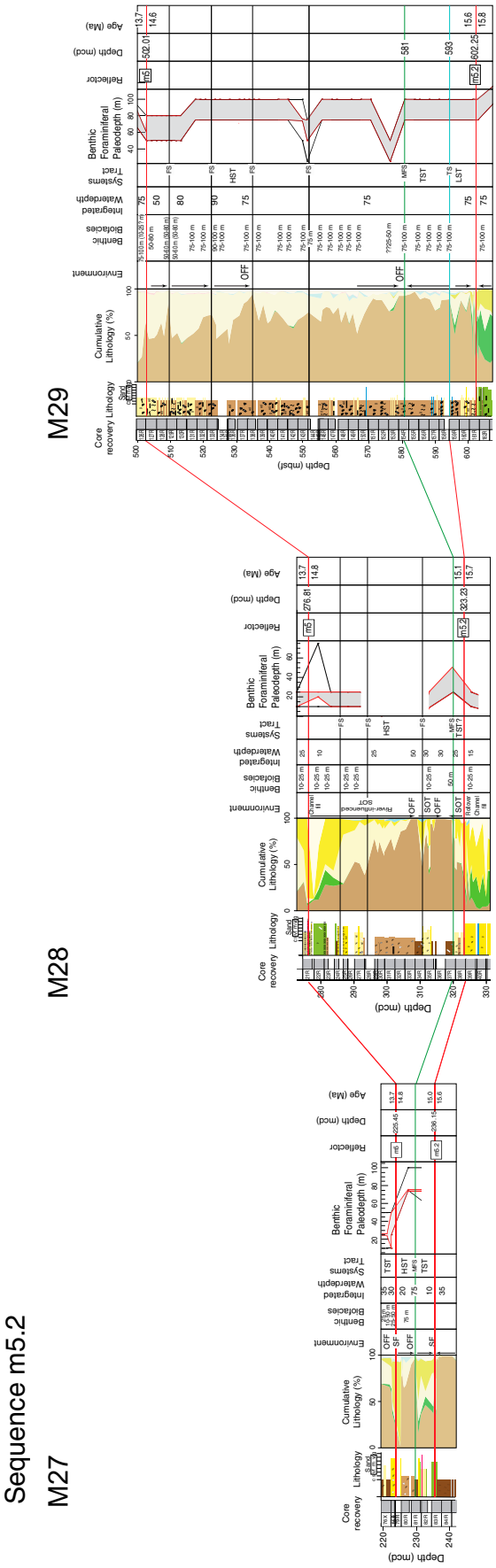

Figure 18. Sequence m5.2 among Integrated Ocean Drilling Program Expedition 313 Sites M27, M28, and M29 showing detailed paleobathymetry and systems tracts based on foraminiferal and lithologic interpretations (see Fig. 13 caption for details and abbreviations).

This may be explained by the fact that the offshore (>30 m paleodepth) clay and silty clays of cores 36 and 37 at Site M28 lack foraminifera >150 µm due to preservation. The foreset of sequence m5.2 at Site M29 is dominated by biofacies that indicate 75–100 m, with some variation.

Sequence m5

At Site M27, sequence m5 (225.45–218.39 mcd; 13.7–13.6 Ma) is thin, truncated, and fines upsection, deepening from shoreface to offshore, and is interpreted as a TST. Benthic foraminiferal assemblages are characterized by *P. pizarrensis*, indicating that paleodepths were ~25–50 m in the 4 samples examined (Figs. 4–6).

At Site M28, sequence m5 (276.81–254.13 mcd; 13.7–13.5 Ma) was deposited on a topset and coarsens upsection. This is interpreted as an HST, with the MFS/TS merged with the sequence boundary (Miller et al., 2013a). Foraminifera were examined only near the base of the sequence (3 samples), and indicate ~10–25 m paleodepth based on high abundances of *H. hughesi* (Figs. 7–9).

Sequence m5 at Site M29 (502.01–478.61 mcd; 13.7–13.6 Ma; 12 samples examined) consists of two coarsening-upward successions deposited on the lower foreset to bottomset. The lowermost sample examined (501.73 mcd) is dominated by the shallow-water indicator *H. hughesi* (indicating 10–25 m), but the presence of deeper water taxa (*B. gracilis* ~9.5%, *C. pachyderma* 7%) in the same sample indicate deposition at a greater paleodepth (~50–60 m) with downslope transport (Figs. 10–12). The factor 1 biofacies (*Uvigerina* spp.) characterizes most of sequence m5, with both the shallower water *H. hughesi* and the deeper water *C. pachyderma* occurring in relatively high abundances in several of these samples, indicating ~75–100 m paleodepth. There are barren samples scattered through this sequence. There is little indication of variation in paleodepth, so systems tracts interpretations were not made.

Sequence m4.5

Sequence m4.5 at Site M27 (218.39–209 mcd; 13.5–13.2 Ma; 7 samples examined) was deposited on a topset and fines upsection to ~217 mcd in a TST and coarsens above in an HST. It is characterized by the factor 3 biofacies (*P. pizarrensis*, *Hanzawaia* sp. 1, and *H. hughesi*), indicating paleowater depths of 10–50 m (Figs. 4–6). Based on higher abundances of *Hanzawaia* sp. 1 and *H. hughesi*, 213.86 and 212.66 mcd are interpreted as ~25 m paleodepth; the absence of these two species, and the abundant *P. pizarrensis* (46%) indicate

25–50 m at 210.665 mcd. There are also barren samples in this sequence.

At Site M29, sequence m4.5 (478.61–408.65 mcd; 13.6–13.3 Ma; 42 samples examined) was deposited at very high sedimentation rates (>200 m/m.y.) on a truncated foreset (Fig. 2). It consists of a lower coarsening-upward regressive LST succession to 470 mcd. This section yields 2 barren samples near the base (477.08 and 475.58 mcd), overlain by the shallow-water *H. hughesi* biofacies (factor 4; 10–25 m paleodepth; 474.38 mcd; Figs. 10–12). Samples at 473.01 and 470.99 mcd are slightly deeper, characterized by both the *H. hughesi* and *P. pizarrensis* biofacies (factors 4 and 5), likely indicating ~25 m paleodepth (within the 10–50 m range indicated by the combination of the two biofacies). We place a TS at 470 mcd at the top of the regressive succession, based on lithology and foraminifera, with a paleodepth estimate of 50–75 m for 469.91 mcd based on high abundances of *P. pizarrensis* (21%) and *Uvigerina* spp. (21%), along with 11% *B. gracilis* (Figs. 10–12). The *Lenticulina* spp. biofacies (factor 2) that characterizes several samples (473.01 and 466.86 mcd) may indicate downslope transport. Foraminifera are sparse in the three overlying samples (468.36, 466.86, 463.86 mcd), and no paleodepth determination was made (Figs. 10–12). Above this (460.79, 459.21, and 457.71 mcd), high loadings on the factor 5 biofacies (*P. pizarrensis*) and factor 3 biofacies (*B. gracilis*, *B. paula*, and *Hanzawaia* sp. 1) indicate paleodepths near the transition between the two biofacies. We assign a paleodepth of 40–50 m to 460.79 mcd based on the absence of *Uvigerina* spp. from this sample. The presence of *Uvigerina* spp. (~6%–9%) indicates slightly deeper paleodepths at 459.21 and 457.71 mcd (40–60 m).

The deepest paleodepths (75–100 m) in sequence m4.5 at Site M29 are recorded in 4 samples from 455.57 to 451.65 mcd, as indicated by high loadings on the factor 1 biofacies (*Uvigerina* spp.; Figs. 10–12). The MFS is placed at 448 mcd. Together, the TS and MFS bracket a fining-upward TST (470–448 mcd) with the deepest water biofacies of the sequence.

Much of the thick silty HST at Site M29 yields few or no benthic foraminifera below 413.50 mcd; nonetheless, paleobathymetric estimates can be determined for some of the samples. Overlying the MFS (448 mcd), a sample at 447.32 mcd is dominated by *Lenticulina* spp. (63.5%); based on 6%–14% each of *P. pizarrensis*, *B. gracilis*, *B. floridana*, and *Uvigerina* spp., we estimate 25–75 m paleodepth for this sample (Figs. 10–12). Similarly, a sample with *Lenticulina* spp. (86%) and *P. pizarrensis* (14%) is estimated as 10–50 m paleodepth. Samples from 442.56 to 433.29 mcd were barren or yielded too few specimens to provide a paleobathymetric estimate.

Benthic foraminifera indicate that most of the remainder of the HST in sequence m4.5 was deposited in the middle-middle neritic zone, with varying abundances of *B. gracilis* and *B. paula* indicating 50–80 m paleodepth (Figs. 10–12). This section includes sporadic barren samples, and a section of barren samples from 419.60 to 415.07 mcd. In contrast, abundant foraminifera from 413.50 to 410.80 mcd support a 50–80 m paleodepth in the HST, suggesting an FS at ~430 mcd.

Sequence m4.4

Sequence m4.4 at Site M29 (409.27–377.15 mcd; 13.3–13.2 Ma; 23 samples examined) sampled a highly truncated foreset that consists of silt and silty clay capped by a few sand beds, deposited at very high sedimentation rates (>300 m/m.y.). A shallowing to 25–50 m paleodepth in the lowermost portion of the sequence (408.90 mcd) is indicated by the *P. pizarrensis* biofacies (factor 5; Figs. 10–12); this is consistent with the interpretation that these sediments were deposited at the shallowest depths of the offshore zone (Mountain et al., 2010). Similar to the upper portion (HST) of the underlying m4.5 sequence, much of sequence m4.4 is characterized by the factor 3 biofacies (*B. gracilis*, *B. paula*, and *Hanzawaia* sp. 1), indicating 50–80 m paleodepth (Figs. 10–12). Two closely spaced samples in the lower part of the sequence (404.35 and 404.32 mcd) may indicate slightly shallower paleodepths (25–80 m), as indicated high abundances of *P. pizarrensis* (67%–69%), in addition to *B. gracilis* (8%–17%); however, this paleodepth estimate is not well constrained because the samples yielded sparse foraminifera (10–17 specimens). This sequence includes sporadic barren samples.

Sequence m4.3

Sequence m4.3 (377.15–364.86 mcd; 13.2–13.1 Ma; 8 samples examined) at Site M29 is highly truncated. The *B. gracilis* biofacies (factor 3) indicates that the lower portion of this sequence was deposited at 50–80 m paleodepth (376.76–372.36 mcd; Figs. 10–12). The remaining samples in this sequence yield rare benthic (*B. gracilis* or *Lenticulina* spp., 1–3 specimens) and/or rare planktonic (1–5 specimens) foraminifera, providing insufficient basis for a paleobathymetric estimate.

Sequence m4.2-4.1

At Site M29, sequence m4.2 (364.86–342.81 mcd; 13.1–13.0 Ma; 16 samples examined) is heavily eroded, and consists of two coarsening-upward successions that appear to be parasequences within the LST. The lower parasequence (9 samples from 364.70 to 350.99 mcd, excluding 2 barren samples) is characterized by the *P. pizarrensis* biofacies (factor 5), indicating 25–50 m paleodepth; the lowermost sample (364.70 mcd) may be slightly shallower, as indicated by *H. hughesi* and *P. pizarrensis*, indicating 10–50 m paleodepth (Figs. 10–12). The higher abundance of *Uvigerina* spp. (9%) at 353.71 mcd may indicate deposition toward the lower end of this depth range (50 m). Samples in the upper parasequence are barren (344.12–349.62 mcd).

The m4.1 surface (343.81 mcd; 13.0 Ma) is most likely a merged sequence boundary–TS (36 samples were examined above m4.1). Benthic foraminiferal assemblages support this interpretation, with the *Uvigerina* spp. biofacies (factor 1) indicating paleodepths of 75–100 m above reflector m4.1 (338.81–335.76 mcd; Figs. 10–12). This section is interpreted as a thin TST, with the MFS at ~340–335 mcd. Two samples that overlie the TST yield foraminifera that indicate shallower depths, consistent with this section being the base of a regressive HST (Figs. 10–12). At 334.23 mcd, the paleodepth is estimated at 40–60 m, reflecting the abundances of *P. pizarrensis* (25%) and *Uvigerina* spp. (17.5%). At 332.71 mcd, an increase in *P. pizarrensis* (65%) indicates a shallower paleodepth (25–50 m). The remainder of the HST yields only barren samples. Estimates of distance from shoreline based on palynomorphs are consistent with the detailed paleobathymetric variations in m4.4–m4.1 (McCarthy et al., 2013).

Sequences m4.4, m4.3, m4.2, and m4.1 merge landward of Site M29, and the m4.1-4.4 concatenated sequence boundary occurs at 209 mcd at Site M27. Nearly all the samples examined for foraminifera above this sequence boundary were barren (8 samples from 208.99 to 195.62 mcd). A single sample (204.13 mcd) yields an assemblage (11.4% *P. pizarrensis*, 14.3% *B. gracilis*, 54.3% *Buliminella curta*) that indicates 25–80 m paleodepth; we tentatively narrow this estimate to 50–80 m, based on the abundance of *Buliminella* (Figs. 4–6).

DISCUSSION

Our Expedition 313 samples yield predominantly in situ biofacies, although there are several excellent examples of mixing of downslope-transported specimens within deep-water (75–120 m) deposits. Examples include sequence m5.4–1 at Site M28, and sequences m5.47, m5.3, m5.2, and m5 at Site M29. Downslope transport is most prevalent at Site M29, which primarily sampled bottomsets older

than sequence m5 (older than 14.6 Ma) and truncated foresets younger than sequence m5 (younger than 13.7 Ma). At Site M29, Sr isotope analyses also indicate extensive reworking and downslope transport in sediments younger than ca. 15 Ma; however, sediments older than 15 Ma show less pervasive reworking, according to Sr isotope analyses (Browning et al., 2013).

The deepest water in situ biofacies at the Expedition 313 sites occur in bottomsets of the clinothems and the lower portions of the foresets. At Site M27, the Eocene–earliest Oligocene bottomsets (>617 mcd) yield the deepest water biofacies (100–120 m; Figs. 2 and 6). The overlying bottomset sequences are slightly shallower, but are still relatively deep (75–100 m for 617–509 mcd; 50–80 m for 500.06 mcd). Sequence m5.8 was sampled on the foreset in the thickest part of the clinothem at Site M27 (beneath the m5.7 rollover; Fig. 2), with a zone of maximum flooding (467.01–421.31 mcd) characterized by biofacies indicating 50–80 m paleodepth. The deepest water biofacies at Site M28 occurs within the thick foreset of sequence m5.4 (Figs. 2 and 9) and on bottomsets. At Site M29, the deepest water biofacies also occur in the bottomsets and/or foresets, in and below the lower portion of sequence m4.5 (Figs. 2 and 12). Above these paleodepth maxima, the long-term paleobathymetric reconstructions show an overall shallowing-upward trend as sediment accumulation resulted in reduced accommodation space.

Short-term paleodepth fluctuations punctuate the long-term shallowing-upward successions at the Expedition 313 sites. On the topset of Site M27, a rapid deepening that occurs in sequence m5.3 continues into sequence m5.2, with biofacies that indicate unexpectedly deep paleodepths of ~75–80 m (*Uvigerina* spp.), consistent with estimates of distance from shoreline based on palynomorphs (McCarthy et al., 2013). Biofacies at Site M29 also record a deepening in sequence m5.3 (from 75–100 m to 100–120 m). At Site M28, biofacies indicate a deepening in the lower part of sequence m5.2 (from 10–25 m to 25–50 m). Sequences m5.3 and m5.2 were deposited during the Middle Miocene Climatic Optimum, when global sea level was likely relatively high (see Browning et al., 2013, for comparison of Expedition 313 sequences with the global oxygen isotope curve), suggesting that this deepening had a global cause.

Shallower biofacies characterize progradation that occurred above sequence m5.2 as the clinothems built up and accommodation space decreased (Figs. 2, 6, 9, 12, and 18). Site M29 sampled the post-m5.2 sequences on truncated foresets (Fig. 2), where biofacies indicate a decrease in overall paleodepth to 50–80 m in the upper parts of sequences m4.5 and m4.4, with further shallowing to 25–50 m in sequences m4.3 and m4.2. The exception to this shoaling-upward trend is sequence m4.1 at Sites M27 and M29, which yield biofacies that indicate water depths of 50–80 m and 75–100 m, respectively; this is ~50 deeper than the underlying sequences, and suggests that a regional flooding event occurred at this time. The event was brief, with biofacies indicating a return to shallower depths in sequence m4.1 (25–50 m at M29; barren samples at M27). The sequence m4.1 boundary correlates with the Miocene isotope event Mi4 $\delta^{18}O$ increase (Browning et al., 2013), an ~40 m glacioeustatic lowering based on Mg/Ca and $\delta^{18}O$ (Westerhold et al., 2005). Sea level rose rapidly (0.1–0.2 m.y.) following Mi4, but only by ~25 m (Westerhold et al., 2005). Therefore, the regional flooding event must be due to either regional subsidence (unlikely, because the event was so rapid) or a decrease in sedimentation rate. Seismic profiles show that extensive bypassing occurred at Sites M27–M29 above sequence m4.1 (Karakaya, 2012), suggesting that the increased water depths were due to sediment starvation.

Similar brief paleodepth changes are indicated by shallow biofacies punctuating sections otherwise characterized by deeper biofacies. Some of the shallow excursions correspond well with the oxygen isotopic compilation that indicates relatively low global sea level (see Browning et al., 2013). These include samples at or near sequence boundaries, which in most cases correspond to global sea-level lowering, including Site M29 sequence boundaries m5.7, m5.6, m5.45, m4.5, m4.4, and m4.2 (Fig. 12). In the thick m5.2 sequence, two brief shallowings appear to correspond to $\delta^{18}O$ increases ca. 15.1 and 15.3 Ma.

CONCLUSIONS

Biofacies at all three Expedition 313 sites indicate a long-term shallowing-upward trend as clinothems built seaward and accommodation filled up from the latest Eocene to middle Miocene (Figs. 6, 9, and 12). The bottomsets of the clinothems and the lower portions of the foresets (thick parts of clinothems, under the rollover) yield the deepest water biofacies. The upper portions of the foresets and the topsets are characterized by shallower biofacies, as the accommodation decreased as sediment accumulated (Figs. 13–18).

Superimposed on this, short-term variations in paleowater depth, indicated by integrated biofacies and lithofacies, are likely linked to global sea-level changes indicated by the global oxygen isotope curve. A regional signal is apparent during Mi4, when extensive bypassing and sediment starvation above sequence m4.1 (Karakaya, 2012) resulted in increased water depths.

We used our paleobathymetric reconstructions in a sequence stratigraphic framework to evaluate systems tracts within several early to early-middle Miocene (ca. 23–13 Ma) prograding clinothems sampled at the Expedition 313 sites. Sites M27 and M28 are dominated by TST and HST deposits, with limited LST sediments. Foresets contain all three systems tracts, but tend to be dominated by TST and HST deposition at all three sites. Flooding surfaces associated with parasequence boundaries occur in all systems tracts. Topsets are characterized by TSTs and HSTs.

ACKNOWLEDGMENTS

We thank the drillers and scientists of Integrated Ocean Drilling Program (IODP) Expedition 313 for their enthusiastic collaboration, the Bremen IODP Core Repository for hosting our studies, and B. King, K. Monahan, and H. Smith for laboratory work. Funding was supplied by the U.S. Science Support Program Consortium for Ocean Leadership and samples were provided by the IODP and the International Continental Scientific Drilling Program (ICDP). We thank Jean-Noel Proust, Robert Speijer, and an anonymous reviewer for comments that helped to improve this manuscript.

REFERENCES CITED

Abbott, S.T., and Carter, R.M., 1994, The sequence architecture of mid-Pleistocene (0.35–0.95 Ma) cyclothems from New Zealand: Facies development during a period of known orbital control on sea-level cyclicity, *in* de Boer, P.L., and Smith, D.G., eds., Orbital forcing and cyclic sequences: International Association of Sedimentologists Special Publication 19, p. 367–394, doi:10.1002/9781444304039.ch23.

Abreu, V.S., and Haddad, G.A., 1998, Glacioeustatic fluctuations: The mechanism linking stable isotope events and sequence stratigraphy from the early Oligocene to middle Miocene, *in* de Graciansky, P.-C., et al., eds., Mesozoic and Cenozoic sequence stratigraphy of European Basins: SEPM (Society for Sedimentary Geology) Special Publication 60, p. 245–259; doi:10.2110/pec.98.02.0245.

Austin, J.A., and 27 others, 1998, Initial reports of the Ocean Drilling Program, Leg 174A: College Station, Texas, Ocean Drilling Program, 324 p., doi:10.2973/odp.proc.ir.174a.1998.

Bandy, O.L., 1960, General correlation of foraminiferal structure with environment: International Geological Congress, 21st Session, Copenhagen, Reports, Part 22, p. 7–19.

Boersma, A., 1984, Handbook of common Tertiary *Uvigerina*: Stony Point, New York, Microclimates Press, 207 p.

Browning, J.V., Miller, K.G., and Olsson, R.K., 1997, Lower to middle Eocene benthic foraminiferal biofacies, lithostratigraphic units, and their relationship to sequences, New Jersey Coastal Plain, *in* Miller, K.G., and Snyder, S.W., eds., Proceedings of the Ocean Drilling Program, Scientific results, Volume 150X: College Station, Texas, Ocean Drilling Program, p. 207–228, doi:10.2973/odp.proc.sr.150X.333.1997.

Browning, J.V., Miller, K.G., Sugarman, P.J., Barron, J., McCarthy, F.M.G., Kulhanek, D.K., Katz, M.E., and Feigenson, M.D., 2013, Chronology of Eocene–Miocene sequences on the New Jersey shallow shelf: Implications for regional, interregional, and global correlations: Geosphere, v. 9, doi:10.1130/GES00857.1.

Christie-Blick, N., and Driscoll, N.W., 1995, Sequence stratigraphy: Annual Review of Earth and Planetary Sciences, v. 23, p. 451–478, doi:10.1146/annurev.ea.23.050195.002315.

Christie-Blick, N., Mountain, G.S., and Miller, K.G., 1990, Seismic stratigraphic record of sea-level change, *in* Sea-level change: National Research Council Studies in Geophysics: Washington, D.C., National Academy Press, p. 116–140.

Culver, S.J., and Buzas, M.A., 1980, Distribution of recent benthic foraminifera off the North American Coast: Smithsonian Contributions to Marine Science no. 6, 512 p., doi:10.5479/si.01960768.6.1

Cushman, J.A., and Cahill, E.D., 1933, Miocene foraminifera of the coastal plain of the eastern United States: U.S. Geological Survey Professional Paper 175-A, 50 p.

Eberli, G.P., and 27 others, 1997, Proceedings of the Ocean Drilling Program, Initial reports, Leg 166: College Station, Texas, Ocean Drilling Program, 373 p., doi:10.2973/odp.proc.ir.166.1997.

Gibson, T.G., 1983, Key foraminifera from upper Oligocene to lower Pleistocene strata of the central Atlantic coastal plain: Smithsonian Contributions for Foraminiferal Research, v. 53, p. 355–453.

Greenlee, S.M., Schroeder, F.W., and Vail, P.R., 1988, Seismic stratigraphic and geohistory analysis of Tertiary strata from the continental shelf off New Jersey—Calculation of eustatic fluctuations from stratigraphic data, *in* Sheridan, R., and Grow, J., eds., The Atlantic continental margin: U.S.: Boulder, Colorado, Geological Society of America, The Geology of North America, v. I-2, p. 437–444.

Greenlee, S.M., Devlin, W.J., Miller, K.G., Mountain, G.S., and Flemings, P.B., 1992, Integrated sequence stratigraphy of Neogene deposits, New Jersey continental shelf and slope: Comparison with the Exxon model: Geological Society of America Bulletin, v. 104, p. 1403–1411, doi:10.1130/0016-7606(1992)104<1403:ISSOND>2.3.CO;2.

Grimsdale, T.F., and van Morkhoven, F.P.C.M., 1955, The ratio between pelagic and benthonic foraminifera as a means of estimating depth of deposition of sedimentary rocks: Proceedings of the Fourth World Petroleum Congress Section I/D, p. 474–491.

Haq, B.U., Hardenbol, J., and Vail, P.R., 1987, Chronology of fluctuating sea levels since the Triassic (250 million years ago to present): Science, v. 235, p. 1156–1167, doi:10.1126/science.235.4793.1156.

Hathaway, J.C., Poag, C.W., Valentine, P.C., Miller, R.E., Schultz, D.M., Manheim, R.T., Kohout, F.A., Bothner, M.H., and Sangrey, D.A., 1979, U.S. Geological Survey core drilling on the Atlantic shelf: Science, v. 206, p. 515–527, doi:10.1126/science.206.4418.515.

Inwood, J., Lofi, J., Davies, S., Basile, C., Bjerum, C., Mountain, G., Proust, J.-N., Otsuka, H., and Valppu, H., 2013, Statistical classification of log response as an indicator of facies variation during changes in sea level: Integrated Ocean Drilling Program Expedition 313: Geosphere, v. 9, p. 1025–1043, doi:10.1130/GES00913.1.

Karakaya, S., 2012, Quantitative seismic attribute analysis using artificial neural networks and seismic stratigraphic interpretation of lower to middle Miocene sediments offshore New Jersey [M.S. thesis]: Piscataway, New Jersey, Rutgers University, 205 p.

Katz, M.E., Miller, K.G., and Mountain, G.S., 2003a, Biofacies and lithofacies evidence for paleoenvironmental interpretations of upper Neogene sequences on the New Jersey continental shelf (ODP Leg 174A), *in* Olson, H.C., and Leckie, R.M., eds., Micropaleontologic proxies for sea-level change and stratigraphic discontinuities: SEPM (Society for Sedimentary Geology) Special Publication 75, p. 131–146, doi:10.2110/pec.03.75.0131

Katz, M.E., Tjalsma, R.C., and Miller, K.G., 2003b, Oligocene bathyal to abyssal benthic foraminifera of the Atlantic Ocean: Micropaleontology, v. 49, supplement 2, p. 1-45.

Kolla, V., Biondi, P., Long, B., and Fillar, R., 2000, Sequence stratigraphy and architecture of the late Pleistocene Lagniappe delta complex, northeast Gulf of Mexico, *in* Hunt, D., and Gawthorp, R.L., eds., Sedimentary responses to forced regressions: Geological Society of London Special Publication 172, p. 291–327, doi:10.1144/GSL.SP.2000.172.01.14.

Kominz, M.A., Browning, J.V., Miller, K.G., Sugarman, P.J., Misintseva, S., and Scotese, C.R., 2008, Late Cretaceous to Miocene sea-level estimates from the New Jersey and Delaware coastal plain coreholes: An error analysis: Basin Research, v. 20, p. 211–226.

Loutit, T.S., Hardenbol, J., Vail, P.R., and Baum, G.R., 1988, Condensed section: The key to age determination and correlation of continental margin sequences, *in* Wilgus, C.K., Hastings, B.S., Kendall, C.G.St.C., Posamentier, H.W., Ross, C.A., and Van Wagoner, J.C., eds., Sea Level Changes-An Integrated Approach: SEPM (Society for Sedimentary Geology) Special Publication 42, p. 183–213.

McCarthy, F.M.G., Katz, M.E., Kotthoff, U., Browning, J.V., Miller, K.G., Zanatta, R., William, R.H., Drljepan, M., Hesselbo, S., Bjerrum, C., and Mountain, G.S., 2013, Sea-level control of New Jersey margin architecture: Palynological evidence from IODP Expedition 313: Geosphere, doi:10.1130/GES00853.1.

Miall, A.D., 1991, Stratigraphic sequences and their chronostratigraphic correlation: Journal of Sedimentary Petrology, v. 61, p. 497–505, doi:10.1306/D4267744-2B26-11D7-8648000102C1865D.

Miller, K.G., and Katz, M.E., 1987, Eocene benthic foraminiferal biofacies of the New Jersey Transect, *in* Poag, C.W., et al., Initial reports of the Deep Sea Drilling Project, volume 95, p. 267–298, doi:10.2973/dsdp.proc.95.107.1987.

Miller, K.G., and Mountain, G.S., 1994, Global sea-level change and the New Jersey margin, *in* Mountain, G.S., et al., eds., Proceedings of the Ocean Drilling Program, Initial reports, Leg 150: College Station, Texas, Ocean Drilling Program, p. 11–20, doi:10.2973/odp.proc.ir.150.102.1994.

Miller, K.G., Mountain, G.S., Leg 150 Shipboard Party, and Members of the New Jersey Coastal Plain Drilling Project, 1996, Drilling and dating New Jersey Oligocene–Miocene sequences: Ice volume, global sea level, and Exxon records: Science, v. 271, p. 1092–1095, doi:10.1126/science.271.5252.1092.

Miller, K.G., Rufolo, S., Sugarman, P.J., Pekar, S.F., Browning, J.V., and Gwynn, D.W., 1997, Early to middle Miocene sequences, systems tracts, and benthic foraminiferal biofacies, New Jersey coastal plain, *in* Miller, K.G., et al., Proceedings of the Ocean Drilling Program, Scientific results, Volume 150X: College Station, Texas, Ocean Drilling Program, p. 169–186, doi:10.2973/odp.proc.sr.150X.313.1997.

Miller, K.G., Mountain, G.S., Browning, J.V., Kominz, M., Sugarman, P.J., Christie-Blick, N., Katz, M.E., and Wright, J.D., 1998, Cenozoic global sea-level, sequences, and the New Jersey transect: Results from coastal plain and slope drilling: Reviews of Geophysics, v. 36, p. 569–601, doi:10.1029/98RG01624.

Miller, K.G., Browning, J.V., Sugarman, P.J., McLaughlin, P.P., Kominz, M.A., Olsson, R.K., Wright, J.D., Cramer, B.S., Pekar, S.F., and Van Sickel, W., 2003, 174AX leg summary: Sequences, sea level, tectonics, and aquifer resources: Coastal plain drilling, *in* Miller, K.G., et al., eds., Proceedings of the Ocean Drilling Program, Initial reports, Leg 174AX (Supplement): College Station, Texas, Ocean Drilling Program, p. 1–38, doi:10.2973/odp.proc.ir.174axs.104.2003.

Miller, K.G., Kominz, M.A., Browning, J.V., Wright, J.D., Mountain, G.S., Katz, M.E., Sugarman, P.J., Cramer, B.S., Christie-Blick, N., and Pekar, S.F., 2005, The Phanerozoic record of global sea-level change: Science, v. 310, p. 1293–1298, doi:10.1126/science.1116412.

Miller, K.G., Browning, J.V., Mountain, G.S., Bassetti, M.A., Monteverde, D., Katz, M.E., Inwood, J., Lofi, J., and Proust, J.-N., 2013a, Sequence boundaries are impedance contrasts: Core-seismic-log integration of Oligocene–Miocene sequences, New Jersey shallow shelf: Geosphere, v. 9, doi:10.1130/GES00858.1.

Miller, K.G., and 13 others, 2013b, Testing sequence stratigraphic models by drilling Miocene foresets on the New Jersey shallow shelf: Geosphere, v. 9, doi:10.1130/GES00884.1.

Mitchum, R.M., Vail, P.R., and Thompson, S., 1977, Seismic stratigraphy and global changes of sea level: Part 2. The depositional sequence as a basic unit for stratigraphic analysis: Section 2. Application of seismic reflection configuration to stratigraphic interpretation, *in* Payton, C.E., ed., Seismic stratigraphy: Applications to hydrocarbon exploration: American Association of Petroleum Geologists Memoir 26, p. 53–62.

Monteverde, D.H., Mountain, G.S., and Miller, K.G., 2008, Early Miocene sequence development across the New Jersey margin: Basin Research, v. 20, p. 249–267, doi:10.1111/j.1365-2117.2008.00351.x.

Mountain, G., and Monteverde, D., 2012, If you've got the time, we've got the depth: The importance of accurate core-seismic correlation: American Geophysical Union Fall Meeting, abstract PP51B-2111.

Mountain, G.S., and 27 others, 1994, Proceedings of the Ocean Drilling Program, Initial reports, Volume 150: College Station, Texas, Ocean Drilling Program, 885 p., doi:10.2973/odp.proc.ir.150.1994.

Mountain, G.S., Proust, J.-N., McInroy, D., Cotterill, C., and the Expedition 313 Scientists, 2010, Proceedings of the Integrated Ocean Drilling Program, Expedition 313: Tokyo, Integrated Ocean Drilling Program Management International, Inc., doi:10.2204/iodp.proc.313.2010.

Murray, J.W., 1991, Ecology and Palaeoecology of Benthic Foraminifera: New York, Wiley and Sons, Inc.

Natland, M.L., 1933, The temperature and depth distribution of some recent and fossil foraminifera in the southern California region: Scripps Institution of Oceanography Technical Series, v. 3, p. 225–230.

Neal, J., and Abreu, V., 2009, Sequence stratigraphy hierarchy and the accommodation 849 succession method: Geology, v. 37, p. 779–782.

Olsson, R.K., Melillo, A.J., and Schreiber, B.L., 1987, Miocene sea level events in the Maryland coastal plain and the offshore Baltimore Canyon trough, *in* Ross, C., and Haman, D., eds., Timing and depositional history of eustatic sequences: Constraints on seismic stratigraphy: Cushman Foundation Foraminiferal Research, Special Publication 24, p. 85–97.

Parker, F.L., 1948, Foraminifera of the continental shelf from the Gulf of Maine to Maryland: Harvard Museum of Comparative Zoology Bulletin, v. 100, p. 213–241.

Pekar, S.F., Miller, K.G., and Browning, J.V., 1997, New Jersey Coastal Plain Oligocene sequences, *in* Miller, K.G., et al., Proceedings of the Ocean Drilling Program, Scientific results, Volume 150X: College Station, Texas, Ocean Drilling Program, p. 187–206, doi:10.2973/odp.proc.sr.150X.314.1997.

Poag, C.W., 1977, Foraminiferal biostratigraphy, *in* Scholle, P., ed., Geological studies on the COST no. B-2 well, U.S. Mid-Atlantic outer continental shelf area: U.S. Geological Survey Circular 750, p. 35–36.

Poag, C.W., 1981, Ecologic atlas of benthic foraminifera of the Gulf of Mexico: Stroudsburg, Pennsylvania, Hutchison Ross, 174 p.

Poag, C.W., 1988, Foraminiferal stratigraphy and paleoenvironments of Cenozoic strata cored near Haynesville, Virginia, *in* Mixon, R.B., ed., Geology and paleontology of the Haynesville cores; northeastern Virginia coastal plain: U.S. Geological Survey Professional Paper 1489, p. D1–D31.

Posamentier, H.W., and Vail, P.R., 1988, Eustatic controls on clastic deposition II—Sequence and systems tract models, *in* Wilgus, C.K., Hastings, B.S., Ross, C.A., Posamentier, H.W., Van Wagoner, J.C., and Kendall, C.G.St.C, eds., Sea level changes: An integrated approach: Society of Economic Paleontologists and Mineralogists Special Publication 42, p. 125–154.

Posamentier, H.W., Jervey, M.T., and Vail, P.R., 1988, Eustatic controls on clastic deposition I—Conceptual framework, *in* Wilgus, C.K., et al., eds., Sea level changes: An integrated approach: Society of Economic Paleontologists and Mineralogists Special Publication 42, p. 109–124, doi:10.2110/pec.88.01.0109.

Schlee, J.S., 1981, Seismic stratigraphy of Baltimore Canyon Trough: American Association of Petroleum Geologists Bulletin, v. 65, p. 26–53.

Schnitker, D., 1970, Upper Miocene foraminifera from near Grimesland, Pitt County, North Carolina: North Carolina Department of Conservation and Development Division of Mineral Resources Special Publication 3, 129 p.

Snyder, S.W., Waters, V.J., and Moore, T.L., 1988, Benthic foraminifera and paleoecology of Miocene Pungo River Formation sediments in Onslow Bay, North Carolina continental shelf, *in* Snyder, S.W., ed., Micropaleontology of Miocene sediments in the shallow subsurface of Onslow Bay, North Carolina continental shelf: Cushman Foundation for Foraminiferal Research Special Publication 25, p. 43–95.

Speijer, R.P., van der Zwaan, G.J., and Schmitz, B., 1996, The impact of Paleocene/Eocene boundary events on middle neritic benthic foraminiferal assemblages from Egypt: Marine Micropaleontology, v. 28, p. 99–132, doi:10.1016/0377-8398(95)00079-8.

Steckler, M.S., Mountain, G.S., Miller, K.G., and Christie-Blick, N., 1999, Reconstruction of Tertiary progradation and clinoform development on the New Jersey passive margin by 2-D backstripping: Marine Geology, v. 154, p. 399–420, doi:10.1016/S0025-3227(98)00126-1.

Tjalsma, R.C. and Lohmann, G.P., 1983, Paleocene-Eocene bathyal and abyssal benthic foraminifera from the Atlantic Ocean: Micropaleontology Special Publication number 4, i–iii: New York, The American Museum of Natural History, p. 1–90.

Vail, P.R., Mitchum, R.M., Jr., Todd, R.G., Widmier, J.M., Thompson, S., III, Sangree, J.B., Bubb, J.N., and Hatlelid, W.G., 1977, Seismic stratigraphy and global changes of sea level, *in* Payton, C.E., ed., Seismic stratigraphy—Applications to hydrocarbon exploration, Parts 1–11: American Association of Petroleum Geologists Memoir 26, p. 49–212.

Vail, P.R., Audemard, F., Bowman, S.A., Eisner, P.N., and Perez-Cruz, C., 1991, The stratigraphic signatures of tectonics, eustasy and sedimentology—An overview, *in* Einsele, G., et al., eds., Cycles and events in stratigraphy: Berlin, Springer-Verlag, p. 617–659.

van Morkhoven, F.P.C.M., Berggren, W.A., Edwards, A.S., et al., 1986, Cenozoic cosmopolitan deep-water benthic foraminifera: Pau, France, Elf-Aquitaine, 421 p.

Weimer, P., and Posamentier, H.W., eds., 1993, Siliciclastic sequence stratigraphy: Recent developments and applications: American Association of Petroleum Geologists Memoir 58, 492 p.

West, O.L.O., Leckie, R.M., and Schmidt, M., 1998, Foraminiferal paleoecology and paleoceanography of the Greenhorn Cycle along the southwestern margin of the Western Interior Sea, *in* Dean, W.E., and Arthur, M.A., eds., Stratigraphy and paleoenvironments of the Cretaceous Western Interior Seaway, USA: SEPM (Society for Sedimentary Geology) Concepts in Sedimentology and Paleontology 6, p. 79–99, doi:10.2110/csp.98.06.0079.

Westerhold, T., Bickert, T., and Röhl, U., 2005, Middle to late Miocene oxygen isotope stratigraphy of ODP site 1085 (SE Atlantic): New constrains on Miocene climate variability and sea-level fluctuations: Palaeogeography, Palaeoclimatology, Palaeoecology, v. 217, p. 205–222, doi:10.1016/j.palaeo.2004.12.001.

Winn, R.D., Roberts, H.H., Kohl, B., Fillon, R.H., Bouma, A., and Constans, R.E., 1995, Latest Quaternary deposition on the outer shelf, northern Gulf of Mexico: Facies and sequence stratigraphy from the Main Pass Block 303 shallow core: Geological Society of America Bulletin, v. 107, p. 851–866, doi:10.1130/0016-7606(1995)107<0851:LQDOTO>2.3.CO;2.